NASA Contractor Report 181989

CALIBRATION OF HEWLETT-PACKARD NETWORK ANALYZERS - A PRECISION VIEWPOINT

W. A. Davis and D. M. Keller

VIRGINIA POLYTECHNIC INSTITUTE
AND STATE UNIVERSITY
Blacksburg, Virginia

Contract NAS1-18106
March 1990

National Aeronautics and
Space Administration

Langley Research Center
Hampton, Virginia 23665-5225

TABLE OF CONTENTS

CHAPTER 1
INTRODUCTION

In the past two decades, the measurement of S (Scattering) parameters has become progressively more important. This importance stems both from the ease of the basic measurement, particularly over a broad frequency range, and the usefulness of this parameter set in the design process. Measurements have been made to below 1 MHz and are slowly being extended into the millimeter wave spectrum (though measurements in this range are almost by necessity done in an S–parameter format). We, not unsurprisingly, find the calibration process and standards at the heart of such a measurement system.

To calibrate such a system for reflection and transmission measurements, Hewlett–Packard Company (HP) provides a set of standards (originally from Maury Microwave) and related data for calibration. Using the HP procedures, several researchers have found anomalies in the resultant data. A not uncommon phenomena is an air–line with a reflection that shows gain. Admittedly, this gain exceeds unity by less than one percent. However, somewhat by accident, researchers have used slightly different calibration data to represent the standards and found substantially improved results for the airlines.

The purpose of this report is to investigate the full calibration process for the existing HP measurement system. We will begin by reviewing the basic calibration process and measurement system. The approach taken by Hewlett–Packard will be

discussed as the methods are developed. A full model for the system will also be developed. This model may be used to develop full system calibration, including the calibration of the HP "open" circuit reference. This approach has the additional advantage of not requiring the "open" for the calibration, a fact critical to certain measurement environments such as the measurement of dielectric and conductive material samples. In such instances, the calibration must often be done using some alternate procedure such as that presented in this report. More importantly, the basic formalism of the modeling enables a user to develop a calibration procedure tailored to a specific need where the HP procedure is inadequate. Our premise is to improve the HP calibration data and then use the fundamental HP procedure when possible. This will provide a high degree of accuracy if the correct calibration data is available, usually in excess of the accuracy specifications of the HP 8510 network analyzer system.

Sample results will be presented which validate the method and demonstrate the potential errors using HP's process and data. This will include the effects of both fixed terminations and sliding loads on the choice of calibration data used to represent the HP "open" standard. Limitations of the approach will be discussed in addition to assumptions built into the calibration and accuracy process. Associated effects of the assumptions about switching networks have led to alternate procedures requiring a system modification (Speciale, 1977b). Since this latter work is not directly related to the report objective, no consideration will be given to this alternate procedure at this time.

CHAPTER 2
DEVELOPMENT OF 8–PORT MODEL AND DESCRIBING EQUATIONS

The measurement of the S parameters of a device under test (DUT) is to be performed using a HP network analyzer system. The development to be presented is applicable to both the HP8410 and HP8510 series systems, excluding the new TRL calibration technique. The basic variations in the measurements are due in part to each of the following in addition to some other minor factors:

1. Imperfections in coaxial switches used in the system, particularly causing variations between switching periods;
2. System noise;
3. Generator noise;
4. Frequency stability (improved with phase lock);
5. Nonlinearity in detectors (particularly phase detection near the limits);
6. Signal leveling;
7. Quantization errors (in A–to–D conversion).

The basic system is shown in Fig. 1 as used for measurement of s_{11} and s_{21}. To measure s_{22} and s_{12}, either the DUT may be reversed or the source may be switched to the right end of the system. The latter is used for the HP systems and is a random source of error, which may be avoided only with a system modification.

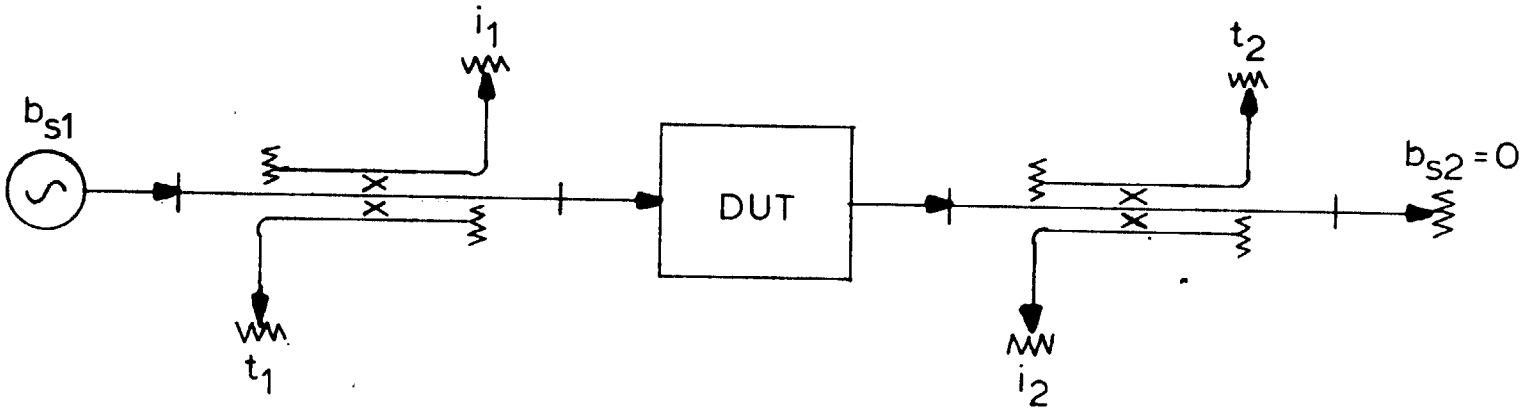

Figure 1. Basic physical layout of S–parameter test system. The i's and t's are internal to the network analyzer.

The modification (Speciale, 1977a) will not be considered in this report. We will find later that the calibration may be done for the system as shown and repeated independently for the system with the source switched to the output. The basic procedures for the two sets of measurements do not interact.

Though Fig. 1 represents the fundamental layout, the actual measurement process is complicated somewhat by possible crosstalk between channels of the network analyzer. A complete 8–port model of the 2–port measurement system with the DUT connected is shown in flow–graph form in Fig. 2. If we observe the details of the measurement system in Fig. 1, we find 8 ports to the outside world: the two source connections, the DUT connections, and the 4 network analyzer terms. The latter have been referred to as terms since they may actually represent voltages internal to the network analyzer which are processed by the network analyzer for the S–parameter estimation.

The network of Fig. 2 may be substantially simplified using either of two basic observations. Since the terminations on the network analyzer ports and source ports (neglecting switching errors) are to be constant at a given frequency (not necessarily zero), they may be imbedded in the S–parameters of a simpler system description. This is a common practice when an n–port is to be used as an (n–m)–port with the extra m ports terminated in fixed loads. The computation requires a bit of matrix algebra. To demonstrate this effect, let us assume the parameters of the 8–port are described by s'_{ij} and port k is terminated in Γ_k. Then the modified s^s_{ij} are given by

$$s^s_{ij} = s'_{ij} + \frac{s'_{ik} s'_{kj} \Gamma_k}{1 - s'_{kk} \Gamma_k} \qquad (1a)$$

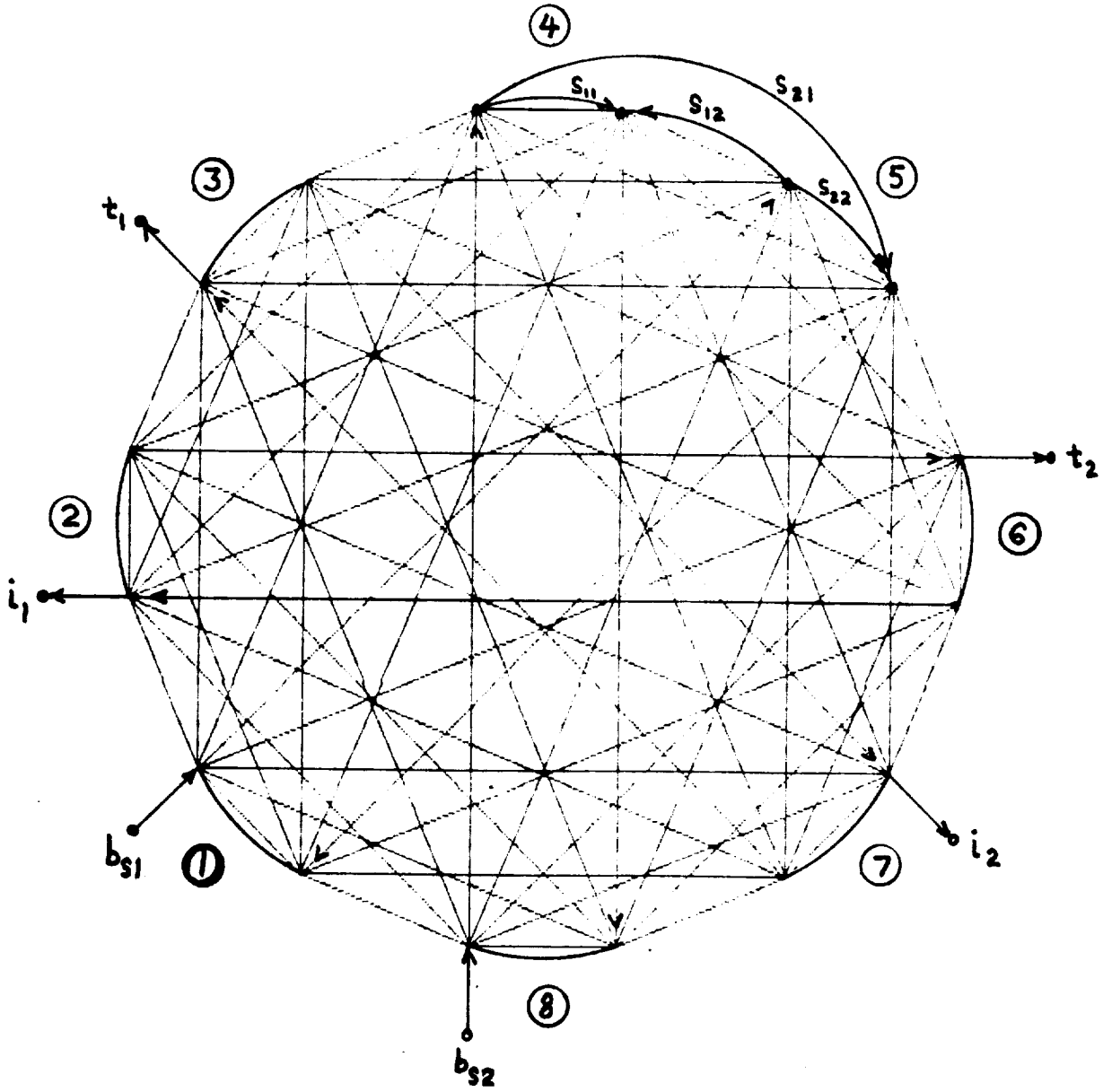

Figure 2. Flow–graph for the system 8–port model.

and

$$s^s_{kj} = \frac{s'_{kj}}{1 - s'_{kk}\,\Gamma_k} \tag{1b}$$

or

$$s^s_{ik} = \frac{1}{1 - s'_{kk}\,\Gamma_k}. \tag{1c}$$

These formulas may be used for each port k which has a constant termination until the full system has been simplified.

An alternative is to note that a similar result may be obtained by using the general form of S–parameters and defining the normalization impedance at each of the constant termination ports to be the constant termination. This approach results in the same form. The actual numbers obtained from the original are unimportant since the true numbers are not known. In fact, the desired result is the form obtained and not the actual numerical relationship of the final model numbers to the original. This form for the 8–port system which describes the HP network analyzer systems is given by the simplified flow graph of Fig. 3. For this form, the final system S–parameters will be denoted by s^s_{ij}, and the relationship to Fig. 2 will be ignored. In this simplified system, only 24 parameters are nonzero. Indeed, if all of the parameters existed, they would have been found to combine in the calibration process to result in another set of 24 terms.

Before we consider the full calibration problem, we will consider the fundamental problem of reflection coefficient measurement of a one–port. In this case only s_{11} of the DUT is nonzero. We will denote this value simply by s. For this measurement, we may set b_{s2} (the second source) to zero and consider only the ratio $\Gamma = (t_1 / i_1)$. In an ideal system, Γ would be equal to s. Our job is to

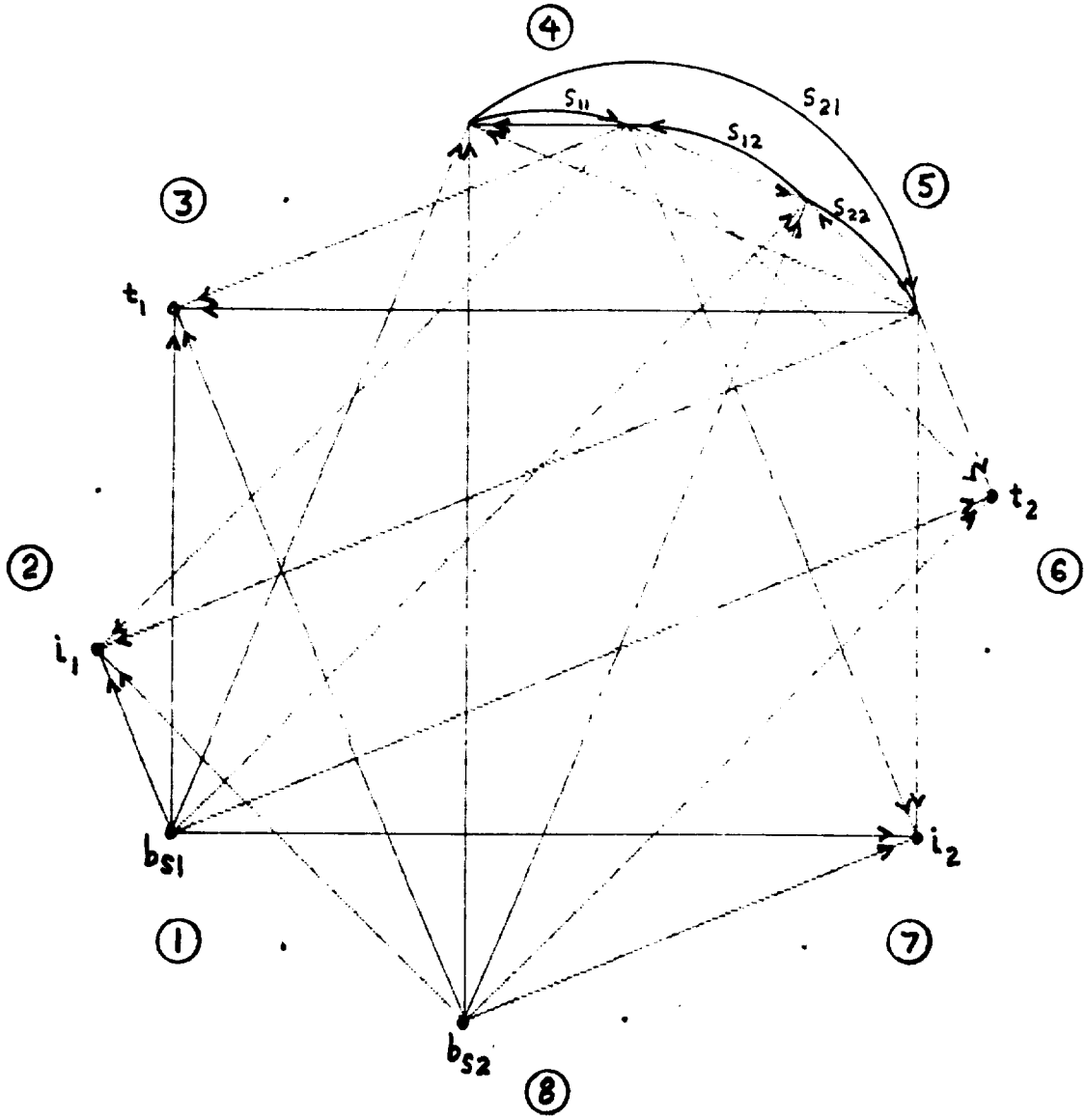

Figure 3. Simplified flow–graph of system 8–port model.

determine the Γ and s relationship so that s may be computed from a measured value of Γ.

In terms of the system S–parameters and s, the measured Γ displayed by the network analyzer will have the value

$$\Gamma = \frac{s^s_{31} + (s^s_{34}\, s^s_{41} - s^s_{44}\, s^s_{31})\, s}{s^s_{21} + (s^s_{24}\, s^s_{41} - s^s_{44}\, s^s_{21})\, s}$$

or equivalently

$$\Gamma = \frac{a_0 + a_1\, s}{1 + b_1\, s}, \tag{2}$$

where the s^s_{ij} are constants and the numerator and denominator have been divided by s^s_{21} which represents the incident coupling to the incident sample port. Since only the ratio Γ is desired, we may simply normalize all signal paths departing the source by the level of coupling to the incident sample port if desired and reduce the number of unknown coefficients by one.

As already suggested, we need to determine the coefficients of (2) in order to compute s from the measured Γ. If we assume that ideal terminations are available, then a_0 is the Γ obtained with a perfect terminating load attached. For the Γ's of a short and open given by Γ_s and Γ_o respectively, then

$$a_1 = \frac{(\Gamma_o + \Gamma_s)\, a_0 - 2\, \Gamma_o\, \Gamma_s}{\Gamma_o - \Gamma_s}$$

and

$$b_1 = \frac{2\, a_0 - \Gamma_o - \Gamma_s}{\Gamma_o - \Gamma_s}.$$

With these terms, then s is simply computed as

$$s = \frac{a_0 - \Gamma}{-a_1 + b_1\, \Gamma}. \tag{3}$$

Thus the basic process for a reflection coefficient s is rather straightforward. The problem arises when we realize that the only near–perfect termination is the short circuit. The load and open are essentially impossible to construct as perfect terminations. This means that a procedure must either be developed which pursues another process of calibration, or the load and open terminations must be made known in some manner. These processes will be the discussion of latter chapters of this report. We stop at this point of the simple reflection problem and begin the more general problem and the necessary calibration procedures in the next chapter.

The full development of the next chapter requires to use of the basic equations for the model of Figure 2. These equations are given by

$$i_1 = s^s_{21}\, b_{s1} + s^s_{24}\, b_1 + s^s_{25}\, b_2 + s^s_{28}\, b_{s2} \qquad (4a)$$

$$t_1 = s^s_{31}\, b_{s1} + s^s_{34}\, b_1 + s^s_{35}\, b_2 + s^s_{38}\, b_{s2} \qquad (4b)$$

$$i_2 = s^s_{71}\, b_{s1} + s^s_{74}\, b_1 + s^s_{75}\, b_2 + s^s_{78}\, b_{s2} \qquad (4c)$$

$$t_2 = s^s_{61}\, b_{s1} + s^s_{64}\, b_1 + s^s_{65}\, b_2 + s^s_{68}\, b_{s2} \qquad (4d)$$

$$a_1 = s^s_{41}\, b_{s1} + s^s_{44}\, b_1 + s^s_{45}\, b_2 + s^s_{48}\, b_{s2} \qquad (4e)$$

$$a_2 = s^s_{51}\, b_{s1} + s^s_{54}\, b_1 + s^s_{55}\, b_2 + s^s_{58}\, b_{s2} \qquad (4f)$$

$$b_1 = s_{11}\, a_1 + s_{12}\, a_2 \qquad (4g)$$

and

$$b_2 = s_{21}\, a_1 + s_{22}\, a_2. \qquad (4h)$$

These equations are combined in the next chapter to obtain a complete description of the measured S–parameters.

CHAPTER 3
CALIBRATION USING IDEAL STANDARDS

As described in the previous chapter, a rigorous development of the system model and resultant equations is easily done. We shall complete the equation development in this chapter and begin the consideration of full system calibration with the use of perfect calibration standards. This development will be extended in later chapters.

3.1 Describing Equations

As shown in the previous chapter, the simplified eight–port model of the network analyzer has eight describing equations. These equations may be combined to obtain equations for only the four measured terms i_1, t_1, i_2, and t_2. It is convenient to define $(\frac{t_1}{i_1}\big|_{b_{s2}=0})$, $(\frac{t_2}{i_1}\big|_{b_{s2}=0})$, $(\frac{t_1}{i_2}\big|_{b_{s1}=0})$, and $(\frac{t_2}{i_2}\big|_{b_{s1}=0})$, denoted s^m_{11}, s^m_{21}, s^m_{12}, and s^m_{22} respectively (the m denoting measured) to represent the four ratios are measured directly by the network analyzer, to obtain

$$
\begin{aligned}
s^m_{11} = \Big\{ & s^s_{31} + (s^s_{34}s^s_{41} - s^s_{31}s^s_{44})\, s_{11} + (s^s_{34}s^s_{51} - s^s_{31}s^s_{54})\, s_{12} \\
& + (s^s_{35}s^s_{41} - s^s_{31}s^s_{45})\, s_{21} + (s^s_{35}s^s_{51} - s^s_{31}s^s_{55})\, s_{22} \\
& + [s^s_{34}\,(s^s_{51}s^s_{45} - s^s_{41}s^s_{55}) + s^s_{35}\,(s^s_{41}s^s_{54} - s^s_{51}s^s_{44}) \\
& + s^s_{31}\,(s^s_{44}s^s_{55} - s^s_{45}s^s_{54})]\, \Delta_s \Big\} \Big/ \Big\{ s^s_{21} + (s^s_{24}s^s_{41} - s^s_{21}s^s_{44})\, s_{11}
\end{aligned}
$$

$$+ (s^s_{24}s^s_{51}-s^s_{21}s^s_{54})\ s_{12} + (s^s_{25}s^s_{41}-s^s_{21}s^s_{45})\ s_{21}$$
$$+ (s^s_{25}s^s_{51}-s^s_{21}s^s_{55})\ s_{22} + [s^s_{24}\ (s^s_{51}s^s_{45}-s^s_{41}s^s_{55})$$
$$+ s^s_{25}\ (s^s_{41}s^s_{54}-s^s_{51}s^s_{44}) + s^s_{21}\ (s^s_{44}s^s_{55}-s^s_{45}s^s_{54})]\ \Delta_s \Big\} \qquad (5a)$$

$$s^m_{21} = \Big\{s^s_{61} + (s^s_{64}s^s_{41}-s^s_{61}s^s_{44})\ s_{11} + (s^s_{64}s^s_{51}-s^s_{61}s^s_{54})\ s_{12}$$
$$+ (s^s_{65}s^s_{41}-s^s_{61}s^s_{45})\ s_{21} + (s^s_{65}s^s_{51}-s^s_{61}s^s_{55})\ s_{22}$$
$$+ [s^s_{64}\ (s^s_{51}s^s_{45}-s^s_{41}s^s_{55}) + s^s_{65}\ (s^s_{41}s^s_{54}-s^s_{51}s^s_{44})$$
$$+ s^s_{61}\ (s^s_{44}s^s_{55}-s^s_{45}s^s_{54})]\ \Delta_s \Big\} \Big/ \Big\{s^s_{21} + (s^s_{24}s^s_{41}-s^s_{21}s^s_{44})\ s_{11}$$
$$+ (s^s_{24}s^s_{51}-s^s_{21}s^s_{54})\ s_{12} + (s^s_{25}s^s_{41}-s^s_{21}s^s_{45})\ s_{21}$$
$$+ (s^s_{25}s^s_{51}-s^s_{21}s^s_{55})\ s_{22} + [s^s_{24}\ (s^s_{51}s^s_{45}-s^s_{41}s^s_{55})$$
$$+ s^s_{25}\ (s^s_{41}s^s_{54}-s^s_{51}s^s_{44}) + s^s_{21}\ (s^s_{44}s^s_{55}-s^s_{45}s^s_{54})]\ \Delta_s \Big\} \qquad (5b)$$

$$s^m_{12} = \Big\{s^s_{38} + (s^s_{34}s^s_{48}-s^s_{38}s^s_{44})\ s_{11} + (s^s_{34}s^s_{58}-s^s_{38}s^s_{54})\ s_{12}$$
$$+ (s^s_{35}s^s_{48}-s^s_{38}s^s_{45})\ s_{21} + (s^s_{35}s^s_{58}-s^s_{38}s^s_{55})\ s_{22}$$
$$+ [s^s_{34}\ (s^s_{58}s^s_{45}-s^s_{48}s^s_{55}) + s^s_{35}\ (s^s_{48}s^s_{54}-s^s_{58}s^s_{44})$$
$$+ s^s_{38}\ (s^s_{44}s^s_{55}-s^s_{45}s^s_{54})]\ \Delta_s \Big\} \Big/ \Big\{s^s_{78} + (s^s_{74}s^s_{48}-s^s_{78}s^s_{44})\ s_{11}$$
$$+ (s^s_{74}s^s_{58}-s^s_{78}s^s_{54})\ s_{12} + (s^s_{75}s^s_{48}-s^s_{78}s^s_{45})\ s_{21}$$
$$+ (s^s_{75}s^s_{58}-s^s_{78}s^s_{55})\ s_{22} + [s^s_{74}\ (s^s_{58}s^s_{45}-s^s_{48}s^s_{55})$$
$$+ s^s_{75}\ (s^s_{48}s^s_{54}-s^s_{58}s^s_{44}) + s^s_{78}\ (s^s_{44}s^s_{55}-s^s_{45}s^s_{54})]\ \Delta_s \Big\} \qquad (5c)$$

and

$$s^m_{22} = \Big\{s^s_{68} + (s^s_{64}s^s_{48}-s^s_{68}s^s_{44})\ s_{11} + (s^s_{64}s^s_{58}-s^s_{68}s^s_{54})\ s_{12}$$
$$+ (s^s_{65}s^s_{48}-s^s_{68}s^s_{45})\ s_{21} + (s^s_{65}s^s_{58}-s^s_{68}s^s_{55})\ s_{22}$$

$$+ [s^s_{64} (s^s_{58}s^s_{45} - s^s_{48}s^s_{55}) + s^s_{65} (s^s_{48}s^s_{54} - s^s_{58}s^s_{44})$$
$$+ s^s_{68} (s^s_{44}s^s_{55} - s^s_{45}s^s_{54})] \Delta_s \Big\} / \Big\{ s^s_{78} + (s^s_{74}s^s_{48} - s^s_{78}s^s_{44})\, s_{11}$$
$$+ (s^s_{74}s^s_{58} - s^s_{78}s^s_{54})\, s_{12} + (s^s_{75}s^s_{48} - s^s_{78}s^s_{45})\, s_{21}$$
$$+ (s^s_{75}s^s_{58} - s^s_{78}s^s_{55})\, s_{22} + [s^s_{74} (s^s_{58}s^s_{45} - s^s_{48}s^s_{55})$$
$$+ s^s_{75} (s^s_{48}s^s_{54} - s^s_{58}s^s_{44}) + s^s_{78} (s^s_{44}s^s_{55} - s^s_{45}s^s_{54})] \Delta_s \Big\}. \qquad (5d)$$

The denominators and and numerators of these equations all have the form $(\alpha_1 + \alpha_2\, s_{11} + \alpha_3\, s_{12} + \alpha_4\, s_{21} + \alpha_5\, s_{22} + \alpha_6\, \Delta_s)$. In addition, Eqs. (5a and b) have the same denominators as do Eqs. (5c and d). This last fact is useful in that the forward and reverse parameter sets may be calibrated and measured independently. In fact if the system user desires to perform the calibration only once, the first two equations may be used for the entire measurement process of a two–port by simply reversing the DUT in the measurement system. To summarize the equations for which the coefficients must be determined, we simply normalize the numerators and denominators of (5) by s^s_{21} and s^s_{78} as appropriate to obtain

$$s^m_{11} = \frac{a_0 + a_1\, s_{11} + a_2\, s_{12} + a_3\, s_{21} + a_4\, s_{22} + a_5\, \Delta_s}{1 + b_1\, s_{11} + b_2\, s_{12} + b_3\, s_{21} + b_4\, s_{22} + b_5\, \Delta_s} \qquad (7a)$$

$$s^m_{21} = \frac{c_0 + c_1\, s_{11} + c_2\, s_{12} + c_3\, s_{21} + c_4\, s_{22} + c_5\, \Delta_s}{1 + b_1\, s_{11} + b_2\, s_{12} + b_3\, s_{21} + b_4\, s_{22} + b_5\, \Delta_s} \qquad (7b)$$

$$s^m_{12} = \frac{d_0 + d_1\, s_{11} + d_2\, s_{12} + d_3\, s_{21} + d_4\, s_{22} + d_5\, \Delta_s}{1 + e_1\, s_{11} + e_2\, s_{12} + e_3\, s_{21} + e_4\, s_{22} + e_5\, \Delta_s} \qquad (7c)$$

and

$$s^m_{22} = \frac{f_0 + f_1\, s_{11} + f_2\, s_{12} + f_3\, s_{21} + f_4\, s_{22} + f_5\, \Delta_s}{1 + e_1\, s_{11} + e_2\, s_{12} + e_3\, s_{21} + e_4\, s_{22} + e_5\, \Delta_s}. \qquad (7d)$$

In a perfect system, these four ratios are precisely equal to s_{11}, s_{21}, s_{12}, and s_{22} respectively. Thus, in a perfect system coefficients a_1, c_3, d_2, and f_4 would be unity and all other coefficients would be zero.

In a practical system, three nonideal effects appear. First, there may be both physical and electrical differences between the reference and test channels, resulting in values of a_1, c_3, d_2, and f_4 unequal to unity. Various user controls (e.g. amplitude and phase controls and line stretchers) are provided in a typical system to compensate for these differences, but the compensation can be made exact for only one frequency and one measured S parameter at a time. Thus, the use of swept–frequency measurements and S parameter test sets sacrifices accuracy for convenience. It is important to note, however, that accurate measurements require only that a_1, c_3, d_2, and f_4 be know as functions of frequency, not that they be set to unity *a priori*.

The second non–ideal effect that may appear is the presence of constant offsets in the measurements (non–zero a_0, c_0, d_0, f_0). These offsets may also be characterized during system calibration and their effects removed to produce accurate measurements. There are usually no user–accessible controls on the equipment to zero them out, although on a polar phase–magnitude (Smith Chart) display the centering adjustments effectively perform this function.

The third non–ideal effect that may appear is crosstalk between parts of the network analyzer due to the finite directivity of the directional couplers and direct radiation (leakage) within the instrument. The mathematical result of this crosstalk is that any or all of the coefficients in the four describing equations may be non–zero. Once again, the values of these coefficients can be found during calibration; now, however, the four equations become coupled with respect to the unknown S parameters of the device, and numerical computation is required to find

the S parameters. (Further, the equations are nonlinear in the S parameters.) It must be borne in mind, however, that the effects of the crosstalk are small in a high–quality system, so that the a_1, c_3, d_2, and f_4 terms are still the dominant terms in their respective equations.

Calibrating the network analyzer system consists of computing the values of the coefficients in the describing equations, based on measurements of known devices. Possible approaches to doing this calibration are discussed in this chapter and the next, starting here with the simplest case —— that of using "perfect" standards.

3.2 Sample Calibration Using Ideal Standards

Assume that the following standard components are available to be measured by the network analyzer:

1) **Perfect shorts**: two short–circuited transmission lines having reflection coefficients $\rho = -1 + j0$.
2) **Perfect opens**: two open–circuited transmission lines having $\rho = 1 + j0$.
3) **Perfect loads**: two terminated transmission lines having $\rho = 0$.
4) **Perfect through line**: a transmission line having no loss, no discontinuities, and zero electrical length.
5) **Perfect half–wave through line**: a transmission line having no loss, no discontinuities, and an electrical length of a half wavelength.

The calibration procedure will be illustrated here by find the a_i, b_i, and c_i, $i = [0,...,5]$, in the describing equations for s_{11}^m and s_{21}^m. These two equations are decoupled from the remaining two describing equations with respect to the coefficients; hence, the two sets can be solved independently for the coefficients. (This statement is not immediately apparent, since the coefficients all depend on the

same set of S parameters $\{s_{ij};\ 1 \leq (i,\ j) \leq 8\}$. The proof will be by construction; i.e., by developing a procedure.)

For reference, the two describing equations whose coefficients are to be found are repeated here:

$$s_{11}^m = \frac{a_0 + a_1 s_{11} + a_2 s_{12} + a_3 s_{21} + a_4 s_{22} + a_5 \Delta_s}{1 + b_1 s_{11} + b_2 s_{12} + b_3 s_{21} + b_4 s_{22} + b_5 \Delta_s} \tag{7a}$$

and

$$s_{21}^m = \frac{c_0 + c_1 s_{11} + c_2 s_{12} + c_3 s_{21} + c_4 s_{22} + c_5 \Delta_s}{1 + b_1 s_{11} + b_2 s_{12} + b_3 s_{21} + b_4 s_{22} + b_5 \Delta_s}. \tag{7b}$$

3.2.1 Step 1

Connect perfect loads to ports 1 and 2 so that

$$S = \begin{bmatrix} 0 & 0 \\ 0 & 0 \end{bmatrix}. \tag{8}$$

Then

$$s_{11}^m = a_0 \tag{9a}$$

and

$$s_{21}^m = c_0. \tag{9b}$$

3.2.2 Step 2

a) Connect a perfect open to port 1 and a perfect load to port 2. Then

$$S = \begin{bmatrix} 1 & 0 \\ 0 & 0 \end{bmatrix} \tag{10}$$

so that

$$s_{11a}^m = \frac{a_0 + a_1}{1 + b_1} \tag{11a}$$

and

$$s_{21a}^m = \frac{c_0 + c_1}{1 + b_1}. \tag{11b}$$

b) Connect a perfect short to port 1 and a perfect load to port 2. Then

$$S = \begin{bmatrix} -1 & 0 \\ 0 & 0 \end{bmatrix} \tag{12}$$

so that

$$s^m_{11b} = \frac{a_0 - a_1}{1 - b_1} \tag{13a}$$

and

$$s^m_{21b} = \frac{c_0 - c_1}{1 - b_1} . \tag{13b}$$

After some algebra, the simultaneous solution of Eqs. (11a) and (13a) is found to be (recall that a_0 is known)

$$a_1 = \frac{a_0 (s^m_{11a} + s^m_{11b}) - 2 s^m_{11a} s^m_{11b}}{s^m_{11a} - s^m_{11b}} \tag{14a}$$

and

$$b_1 = \frac{2 a_0 - (s^m_{11a} + s^m_{11b})}{s^m_{11a} - s^m_{11b}} \tag{14b}$$

Similar expressions result for c_1 and b_1 after solving (11b) and (13b) simultaneously. The two equations for calculating b_1 should give identical results, thus providing a check on measurement and computational techniques. Bear in mind, however, that (s_{21a}) and (s_{21b}) will be very small compared with (s_{11a}) and (s_{11b}); consequently, values of b_1 computed using (s_{11a}) and (s_{11b}) will be less corrupted by measurement noise.

3.2.3 Step 3

a) Connect a perfect load to port 1 and a perfect open to port 2. Then

$$S = \begin{bmatrix} 0 & 0 \\ 0 & 1 \end{bmatrix} \tag{15}$$

so that

$$s^m_{11a} = \frac{a_0 + a_4}{1 + b_4} \tag{16a}$$

and

$$s^m_{21a} = \frac{c_0 + c_4}{1 + b_4} . \tag{16b}$$

b) Connect a perfect load to port 1 and a perfect short to port 2. Then

$$S = \begin{bmatrix} 0 & 0 \\ 0 & -1 \end{bmatrix} \tag{17}$$

so that

$$s^m_{11b} = \frac{a_0 - a_4}{1 - b_4} \tag{18a}$$

and

$$s^m_{21b} = \frac{c_0 - c_4}{1 - b_4} . \tag{18b}$$

Solving simultaneously again yields

$$a_4 = \frac{a_0 (s^m_{11a} + s^m_{11b}) - 2 s^m_{11a} s^m_{11b}}{s^m_{11a} - s^m_{11b}} \tag{19a}$$

and

$$b_4 = \frac{2 a_0 - (s^m_{11a} + s^m_{11b})}{s^m_{11a} - s^m_{11b}} \tag{19b}$$

with similar expressions for c_4 and b_4 in terms of (s^m_{21a}) and (s^m_{21b}).

3.2.4 Step 4

a) Connect perfect opens to ports 1 and 2. Then

$$S = \begin{bmatrix} 1 & 0 \\ 0 & 1 \end{bmatrix} \tag{20}$$

so that

$$s^m_{11a} = \frac{(a_0 + a_1 + a_4) + a_5}{(1 + b_1 + b_4) + b_5} = \frac{\alpha + a_5}{\beta + b_5} \tag{21a}$$

and

$$s^m_{21a} = \frac{(c_0 + c_1 + c_4) + c_5}{(1 + b_1 + b_4) + b_5} = \frac{\gamma + c_5}{\beta + b_5} . \quad (21b)$$

Note that α, β and γ are known.

b) Connect a perfect short in place of the open at port 2. Then

$$S = \begin{bmatrix} 1 & 0 \\ 0 & -1 \end{bmatrix} \quad (22)$$

so that

$$s^m_{11b} = \frac{(a_0 + a_1 - a_4) - a_5}{(1 + b_1 - b_4) - b_5} = \frac{\alpha' - a_5}{\beta' - b_5} \quad (23a)$$

and

$$s^m_{21b} = \frac{(c_0 + c_1 - c_4) - c_5}{(1 + b_1 - b_4) - b_5} = \frac{\gamma' - c_5}{\beta' - b_5} . \quad (23b)$$

Eqs. (21a) and (23a) can be solved simultaneously for a_5 and b_5 as

$$a_5 = \frac{\alpha' s^m_{11a} + \alpha s^m_{11b} - (\beta' + \beta) s^m_{11a} s^m_{11b}}{s^m_{11a} - s^m_{11b}} \quad (24a)$$

and

$$b_5 = \frac{\alpha + \alpha' - \beta s^m_{11a} - \beta' s^m_{11b}}{s^m_{11a} - s^m_{11b}} \quad (24b)$$

Similar equations for c_5 and b_5 result from solving (21b) and (23b) simultaneously.

3.2.5 Step 5

a) Connect ports 1 and 2 with a perfect through line having zero phase shift. Then

$$S = \begin{bmatrix} 0 & 1 \\ 1 & 0 \end{bmatrix} \quad (25)$$

so that

$$s^m_{11a} = \frac{a_0 + (a_2 + a_3) - a_5}{1 + (b_2 + b_3) - b_5} = \frac{\alpha + (a_2 + a_3)}{\beta + (b_2 + b_3)} \quad (26a)$$

and

$$s^m_{21a} = \frac{c_0 + (c_2 + c_3) - c_5}{1 + (b_2 + b_3) - b_5} = \frac{\gamma + (c_2 + c_3)}{\beta + (b_2 + b_3)} . \quad (26b)$$

b) Connect ports 1 and 2 with a perfect through line have 180° phase shift. Then

$$S = \begin{bmatrix} 0 & -1 \\ -1 & 0 \end{bmatrix} \quad (27)$$

so that

$$s^m_{11b} = \frac{a_0 - (a_2 + a_3) - a_5}{1 - (b_2 + b_3) - b_5} = \frac{\alpha' - (a_2 + a_3)}{\beta' - (b_2 + b_3)} \quad (28a)$$

and

$$s^m_{21b} = \frac{c_0 - (c_2 + c_3) - c_5}{1 - (b_2 + b_3) - b_5} = \frac{\gamma' - (c_2 + c_3)}{\beta' - (b_2 + b_3)} . \quad (28b)$$

Solving (26a) and (28a) simultaneously for $(a_2 + a_3)$ and $(b_2 + b_3)$ gives

$$a_2 + a_3 = \frac{\alpha' s^m_{11a} + \alpha s^m_{11b} - (\beta' + \beta) s^m_{11a} s^m_{11b}}{s^m_{11a} - s^m_{11b}} \quad (29a)$$

and

$$b_2 + b_3 = \frac{\alpha + \alpha' - \beta s^m_{11a} - \beta' s^m_{11b}}{s^m_{11a} - s^m_{11b}} . \quad (29b)$$

Similar equations for $(c_2 + c_3)$ and $(b_2 + b_3)$ result from solving (26b) and (29b) simultaneously. Resolving a_2 and a_3, b_2 and b_3, and c_2 and c_3 from their respective sums requires some computation, and is discussed next.

3.3 Solution for a_2, a_3, b_2, b_3, c_2, and c_3

The calibration measurements of the previous section yield values for the following coefficients and sums: a_0, a_1, $(a_2 + a_3)$, a_4, a_5, b_1, $(b_2 + b_3)$, b_4, b_5, c_0, c_1, $(c_2 + c_3)$, c_4, and c_5. The goal of this section is to express a_2, a_3, b_2, b_3, c_2, and c_3 in terms of these known quantities.

We begin by returning to the definitions of the a_i, b_i, and c_i in terms of the network analyzer model [Eqns. (6) and (7)]. Since each of the coefficients of (6) may be divided by either s^s_{21} or s^s_{78} to obtain the form of (7), we will simply let s^s_{21} and s^s_{78} be given by unity in (6). In effect, we are normalizing to s^s_{21} (or s^s_{78}) for every path leading away from port 1 (or port 8) of the network analyzer model.

For convenience, the coefficient definitions are repeated here, incorporating the normalization discussed above:

$$a_0 = s^s_{31} \tag{30a}$$

$$a_1 = s^s_{34}\, s^s_{41} - s^s_{31}\, s^s_{44} \tag{30b}$$

$$a_2 = s^s_{34}\, s^s_{51} - s^s_{31}\, s^s_{54} \tag{30c}$$

$$a_3 = s^s_{35}\, s^s_{41} - s^s_{31}\, s^s_{45} \tag{30d}$$

$$a_4 = s^s_{35}\, s^s_{51} - s^s_{31}\, s^s_{55} \tag{30e}$$

$$a_5 = s^s_{31}\, s^s_{44}\, s^s_{55} - s^s_{55}\, s^s_{34}\, s^s_{41} - s^s_{44}\, s^s_{51}\, s^s_{35} - s^s_{31}\, s^s_{54}\, s^s_{45} + s^s_{45}\, s^s_{34}\, s^s_{51} + s^s_{41}\, s^s_{54}\, s^s_{35} \tag{30f}$$

$$b_0 = 1 \tag{31a}$$

$$b_1 = s^s_{24}\, s^s_{41} - s^s_{44} \tag{31b}$$

$$b_2 = s^s_{24}\, s^s_{51} - s^s_{54} \tag{31c}$$

$$b_3 = s^s_{25}\, s^s_{41} - s^s_{45} \tag{31d}$$

$$b_4 = s^s_{25}\, s^s_{51} - s^s_{55} \tag{31e}$$

$$b_5 = s^s_{44}\, s^s_{55} - s^s_{55}\, s^s_{24}\, s^s_{41} - s^s_{44}\, s^s_{51}\, s^s_{25} - s^s_{54}\, s^s_{45} + s^s_{45}\, s^s_{24}\, s^s_{51} + s^s_{41}\, s^s_{54}\, s^s_{25} \tag{31f}$$

$$c_0 = s^s_{61} \tag{32a}$$

$$c_1 = s^s_{64}\, s^s_{41} - s^s_{61}\, s^s_{44} \tag{32b}$$

$$c_2 = s^s_{64}\, s^s_{51} - s^s_{61}\, s^s_{54} \tag{32c}$$

$$c_3 = s^s_{65}\, s^s_{41} - s^s_{61}\, s^s_{45} \tag{32d}$$

$$c_4 = s^s_{65}\, s^s_{51} - s^s_{61}\, s^s_{55} \tag{32e}$$

and

$$c_5 = s^s_{61}\, s^s_{44}\, s^s_{55} - s^s_{55}\, s^s_{64}\, s^s_{41} - s^s_{44}\, s^s_{51}\, s^s_{65} - s^s_{61}\, s^s_{54}\, s^s_{45} + s^s_{45}\, s^s_{64}\, s^s_{51} + s^s_{41}\, s^s_{54}\, s^s_{65}. \quad (32f)$$

At first it may not appear to be possible to solve for the subscripted constants s_{ij} separately. However, the complete solution may be considered a possibility since we have already obtained 14 measured quantities on which the 14 coefficients depend. If we look even further, we see that we may also set s^s_{41} to unity if desired since it always appears in product with other terms and may be absorbed.

To consider the solution for the additional coefficients, we begin by combining Eqs. (30) – (32) to obtain

$$a_2\, a_3 = a_1\, a_4 - a_0\, a_5 \quad (33a)$$

$$b_2\, b_3 = b_1\, b_4 - b_5 \quad (33b)$$

and

$$c_2\, c_3 = c_1\, c_4 - c_0\, c_5 \quad (33c)$$

with

$$a_2 + a_3 = \gamma_a \quad (34a)$$

$$b_2 + b_3 = \gamma_b \quad (34b)$$

and

$$c_2 + c_3 = \gamma_c. \quad (34c)$$

Since c_2 and c_3 (and similarly a_2, b_2, a_3, and b_3) are the only unknowns in (33c) and (34c), we may solve for them as quadratic forms as

$$c_2 = \frac{\gamma_c}{2} \pm \frac{1}{2}\sqrt{\gamma_c^2 + 4c_1c_4 - 4c_0c_5} \quad (35a)$$

and

$$c_3 = \frac{\gamma_c}{2} - \left(\pm \frac{1}{2}\sqrt{\gamma_c^2 + 4c_1c_4 - 4c_0c_5} \right). \quad (35b)$$

Similar forms occur for a_2, a_3, b_2, and b_3.

The resolution of the (±) is based on the application of physical requirements for the system, specifically that s_{21}^m is dominated by the actual s_{21} of the calibration standard. To this end we may equate c_3 with the larger of the roots in (35) and c_2 with the smaller. The remaining coefficients require a bit more work. We begin by rewriting combinations of (30) through (32) as

$$a_1 - b_1 a_0 = s_{41}\,(s_{34} - s_{24} a_0) \tag{36a}$$

$$a_4 - b_4 a_0 = s_{51}\,(s_{35} - s_{25} a_0) \tag{36b}$$

$$c_1 - b_1 c_0 = s_{41}\,(s_{64} - s_{24} c_0) \tag{36c}$$

and

$$c_4 - b_4 c_0 = s_{51}\,(s_{65} - s_{25} c_0)\,. \tag{36d}$$

We may also combine (34a–c) to obtain

$$\gamma_a - \gamma_b a_0 = s_{51}\,(s_{34} - s_{24} a_0) + s_{41}\,(s_{35} - s_{25} a_0)$$

and

$$\gamma_c - \gamma_b a_0 = s_{51}\,(s_{64} - s_{24} c_0) + s_{41}\,(s_{65} - s_{25} c_0)$$

into which we may substitute (36) to obtain

$$\gamma_a - \gamma_b a_0 = \frac{s_{51}}{s_{41}}\,(a_1 - b_1 a_0) + \frac{s_{41}}{s_{51}}\,(a_4 - b_4 a_0) \tag{37a}$$

$$\gamma_c - \gamma_b c_0 = \frac{s_{51}}{s_{41}}\,(c_1 - b_1 c_0) + \frac{s_{41}}{s_{51}}\,(c_4 - b_4 c_0). \tag{37b}$$

Eqs. (37) provide two forms for s_{51}/s_{41} given by

$$\frac{s_{51}}{s_{41}} = \frac{(\gamma_a - \gamma_b a_0)(c_4 - b_4 c_0) - (\gamma_c - \gamma_b c_0)(a_4 - b_4 a_0)}{(a_1 - b_1 a_0)(c_4 - b_4 c_0) - (c_1 - b_1 c_0)(a_4 - b_4 a_0)} \tag{38a}$$

and

$$\frac{s_{51}}{s_{41}} = \frac{(a_1 - b_1 a_0)(c_4 - b_4 c_0) - (c_1 - b_1 c_0)(a_4 - b_4 a_0)}{(a_1 - b_1 a_0)(\gamma_c - \gamma_b c_0) - (c_1 - b_1 c_0)(\gamma_a - \gamma_b a_0)}. \tag{38b}$$

If we now substitute (32a and b) into 32(c) we obtain

$$c_2 = \left(\frac{s_{51}}{s_{41}}\right) c_1 + c_0 \left(\frac{s_{51}}{s_{41}} s_{44} - s_{54}\right). \tag{39}$$

Only the last term of this expression is unknown at this stage and we may write it as

$$\left(\frac{s_{51}}{s_{41}} s_{44} - s_{54}\right) = \frac{c_2}{c_0} - \frac{s_{51}}{s_{41}} \frac{c_1}{c_0} \tag{40a}$$

and similarly for the c_3 term

$$\left(\frac{s_{41}}{s_{51}} s_{55} - s_{45}\right) = \frac{c_3}{c_0} - \frac{s_{41}}{s_{51}} \frac{c_4}{c_0}. \tag{40b}$$

Forms for the unknown coefficients a_2, a_3, b_2, and b_3 similar to (39) may be written and (40a and b) used to obtain

$$a_2 = \left(\frac{s_{51}}{s_{41}}\right) a_1 + \frac{a_0}{c_0} \left(c_2 - \frac{s_{51}}{s_{41}} c_1\right) \tag{41a}$$

$$a_3 = \left(\frac{s_{41}}{s_{51}}\right) a_4 + \frac{a_0}{c_0} \left(c_3 - \frac{s_{41}}{s_{51}} c_4\right) \tag{41b}$$

$$b_2 = \left(\frac{s_{51}}{s_{41}}\right) b_1 + \frac{1}{c_0} \left(c_2 - \frac{s_{51}}{s_{41}} c_1\right) \tag{41c}$$

and

$$b_3 = \left(\frac{s_{41}}{s_{51}}\right) b_4 + \frac{1}{c_0} \left(c_3 - \frac{s_{41}}{s_{51}} c_4\right). \tag{41d}$$

This completes the solution for the coefficients of (30) to (32). An analogous procedure may be used for the coefficients with an input at port 8.

3.4 Calibration Using Imperfect Standards

The ideal standards envisioned in Section 3.2 do not exist in practice. To the extent that the actual standards differ from the ideal, the task of calibrating the network analyzer becomes more difficult.

The simplest non-ideal case occurs when some or all of the non-zero entries in the S matrix differ from their ideal values of +1 or −1. An example is a standard whose electrical length is incorrect, resulting in a phase angle other than 0° or $\pm 180^\circ$. Mathematically, this case causes little difficulty: the equations relating the measurements $[(s^m_{11a})$ *and* $(s^m_{11b})]$ or $[(s^m_{21a})$ and $(s^m_{21b})]$ to the coefficients a_i and b_i or c_i and b_i generalize to the form

$$s_a = \frac{\alpha + \gamma x}{\beta + \delta y} \tag{42a}$$

and

$$s_b = \frac{\alpha' + \gamma' x}{\beta' + \delta' y} \tag{42b}$$

where α, β, γ, δ, α', β', γ', and δ' are known and x and y are unknown. These equations have the simultaneous solution

$$x = \frac{\alpha' s_a - \alpha \frac{\delta'}{\delta} s_b - (\beta' - \frac{\delta'}{\delta}\beta) s_a s_b}{-\gamma' s_a + \frac{\delta'}{\delta}\gamma s_b} \tag{43a}$$

$$y = \frac{\frac{1}{\delta}[-\alpha\gamma' + \alpha'\gamma + \beta\gamma' s_a - \beta'\gamma s_b]}{-\gamma' s_a + \frac{\delta'}{\delta}\gamma s_b} \tag{43b}$$

It is easy to check that the equations of Steps 1 through 5 in Section 3.2 are special cases of (42a)–(43b). For example, in Step 2a we can identify

$$s_a = s^m_{11a}, \quad \alpha = a_0, \quad \gamma = 1, \quad x = a_1,$$
$$\beta = 1, \quad \delta = 1, \quad y = b_1,$$

and in Step 2b

$$s_b = s^m_{11b}, \quad \alpha' = a_0, \quad \gamma' = -1, \quad x = a_1,$$
$$\beta' = 1, \quad \delta' = -1, \quad y = b_1.$$

The next level of difficulty occurs if the formerly zero entries of S are allowed to be nonzero. One example is the use of an imperfect load having a nonzero reflection coefficient; another example is a through line with discontinuities that make S_{11} or S_{22} nonzero. In this case, the procedures of Section 3.2 are no longer applicable. Instead, the nine test conditions 1 through 5b yield nine simultaneous equations in a_i and b_i, and another nine equations in c_i and b_i. Solution for the unknown a_i and b_i, or for the unknown c_i and b_i, requires solution of a ninth order system of equations. Still, apart from the extra computation there is little difficulty in dealing with this case. The underlying (and perhaps dubious) assumption is, of course, that the S–parameters of the standards are accurately known.

The highest level of difficulty comes about when the characteristics of some or all of the standards are not completely known. An open, for example, might reasonably be expected to have a reflection coefficient of magnitude one (implying no loss), but its phase angle might well be nonzero due to fringing of the electric field at the end of the transmission line. Our proposed techniques for dealing with this last situation are described in the next chapter.

CHAPTER 4
FULL CALIBRATION

The previous chapter discussed ways of calibrating the network analyzer when known standards are available, whether or not those standards are "perfect." This chapter takes up a more difficult problem—how to calibrate the system when the characteristics of the standards are not completely known. We wish to emphasize at the outset that this statement does not imply that the network analyzer can be calibrated accurately using inferior or damaged standard components. Certain assumptions based on their physical properties must be made in order for our proposed method to work. Nevertheless, this method represents a significant theoretical advance over that previously recommended by Hewlett–Packard.

4.1 Standards

We begin by discussing the standards that will be required for this calibration procedure. These standards are all sold by Hewlett–Packard for calibration and verification of their network analyzers. Some of them are not supplied as part of the "basic" calibration kits, however. Thus, implementation of our recommendations might require purchase of additional components that are, admittedly, not inexpensive.

Fortunately, the full procedure described here is necessary only when the standards are not completely known. Once the standards are completely

characterized, the abbreviated calibration procedure of Chapter 3 is adequate provided the standards do not change in their characteristics.

The process can be carried one step further (in face we recommend doing so) by using the full calibration procedure and a set of prime standards to characterize a second set of working standards, to be used for day–to–day calibration with the abbreviated procedure. Thus, one set of prime standards can be maintained for an entire organization employing many network analyzers. An additional advantage is that the prime standards will receive infrequent use, hence will tend to remain in much better physical condition.

To illustrate our calibration scheme, we assume for the remainder of this chapter that the goal is to characterize a set of prime reflection standards and in the process calibrate the network analyzer for reflection measurements at port 1. Using reflection measurements, the working standards can then be characterized.

The required prime standards are as follows:

1. **Perfect short**: As before, we specify that the component have reflection coefficient $\Gamma = -1 + j0$. The phase of 180° is an arbitrary choice to provide a phase reference for the system; in effect this choice locates the reference plane precisely at the shorted end of the transmission line. Since there is no fringing of the TEM wave on a transmission line in the vicinity of a short, there should be no frequency–dependent behavior. The unity magnitude of the reflection coefficient is based on an assumption of losslessness in the component (including its connector). A worn, damaged, or dirty connector will render this assumption invalid. Further, there is no direct way to test the short, since it is being used to calibrate the network analyzer in the first place. For this reason, Hewlett–Packard recommends that all of its precision microwave

standards be verified using sophisticated physical, rather than electrical measurements.

Since some loss, however small, is inevitable in a real–world connector, there may be a legitimate concern about the lossless assumption. The best justification for this assumption is that no better one can be made unless the short is modeled with the material properties used in a skin–depth formulation. This modeling would be based on documented estimates of the material conductivity obtained from cavity resonance measurements. Further, if the physical quality of the standards is very high, it seems reasonable to assume that the loss associated with each mated connector pair is about the same. Under this assumption, the loss of one connector pair can be absorbed into the network analyzer model, so that it is the component beyond the connector that is being characterized.

2. **Lossless open**: We assume that the open has a reflection coefficient close to unity which is consistent with the existing closed region. Because of field fringing near the discontinuity, the precise electrical location of the open end is not known in advance and it exhibits a frequency–dependent behavior. As with the short, the unity magnitude of the reflection coefficient is a consequence of its assumed losslessness.
3. **Two lossless transmission lines of different electrical lengths**: Once again, the lossless property is assumed. There is no need to know the exact lengths of the lines; it is only necessary that they be significantly different.
4. **Sliding load**: This component consists of a transmission line terminated by a block of resistive material. The termination may be slid up and down the transmission line to change its distance from the input connector. Assuming that the termination is of good quality and that it maintains good contact

with the transmission line, the reflection coefficient seen at the input of the line will have a constant magnitude. Its phase, however, will vary with the position of the terminator (load). Thus the input reflection coefficient of the line will be located on a circle in the complex plane.

4.2 Reflection Calibration

Using the precision standards just described, the network analyzer is to be calibrated for reflection (s_{11}) measurements. We assume that port 2 is terminated with a good matched load so that $s_{12} = s_{21} = s_{22} = 0$ (Strictly speaking, this termination is not a requirement, as non–zero s_{12}, s_{21}, and s_{22} may be absorbed in the constants as long as they do not change.) The describing equation of interest is (6a), which reduces to

$$s_{11}^m = \frac{a_0 + a_1 s_{11}}{1 + b_1 s_{11}}. \qquad (44)$$

4.2.1. Shorted line measurements

With the short connected to port 1,

$$s_{11} = -1$$

and

$$s_{11}^m = \frac{a_0 - a_1}{1 - b_1} = \Gamma_s. \qquad (45)$$

If the short is now connected to port 1 through either of the two lossless transmission lines, the input of the transmission line must have s_{11} of the form

$$s_{11} = 1\, e^{j\varphi}, \qquad (46)$$

that is, a reflection coefficient of unity magnitude (because of the lossless nature of the line) but nonzero phase shifts (because of the nonzero lengths of the lines).

Obviously, the short alone is a special case of (46) having $\varphi = 0$.

The measured $s_{11}^m\big|_{short}$, $s_{11}^m\big|_{short1}$, $s_{11}^m\big|_{short2}$ satisfy the equation

$$s_{11i}^m = \frac{a_0 + a_1 e^{j\varphi_i}}{1 + b_1 e^{j\varphi_i}} \tag{47}$$

for each i. It is possible to show that the bilinear transformation relating s_{11}^m to s_{11} maps circles into circles; specifically, if

$$s_{11} = |\Gamma|\ e^{j\theta}, \quad 0 \le \theta < 2\pi \tag{48}$$

then

$$s_{11}^m = C + R\ e^{j\alpha} \tag{49}$$

where

$$C = \frac{a_1}{b_1} + \frac{1 - \frac{a_1}{b_1}}{1 - |b_1|^2\ |\Gamma|^2} \tag{50a}$$

$$R = \frac{|a_0\ b_1 - a_1|\ |\Gamma|}{1 - |b_1|^2\ |\Gamma|^2} \tag{50b}$$

Thus, connecting the short through various lengths of lossless line produces measurement points that lie on the circle given by (49)–(50) with $|\Gamma| = 1$. A minimum of three points is needed to determine the circle uniquely. These points, as discussed above, can be found by measuring the short alone, and the short with two different lengths of lossless line. (As an alternative and improvement, the short, the open, and both the short and the open on a lossless line can be used for determining the above circle. This approach circumvents some of the problems which arise due to loss in the line extensions.)

The circle in the s_{11}^m plane that results from these measurements will be

denoted

$$s^m_{11s} = C_s + R_s\, e^{j\alpha_s} \tag{51}$$

with

$$C_s = \frac{a_1}{b_1} + \frac{a_0 - \frac{a_1}{b_1}}{1 - |b_1|^2}$$

$$= \frac{a_0 - a_1\, b_1^*}{1 - |b_1|^2} \tag{52a}$$

and

$$R_s = \frac{|a_0\, b_1 - a_1|}{1 - |b_1|^2}. \tag{52b}$$

4.2.2. Sliding load measurements

At the input of the sliding load

$$s^m_{11} = \epsilon\, e^{j\varphi_\ell} \tag{53}$$

where $0 \leq \epsilon \leq 1$. Measuring the sliding load for various positions of the termination gives values of s^m_{11} satisfying

$$s^m_{11} = \frac{a_0 + a_1\, \epsilon\, e^{j\varphi_\ell}}{1 + b_1\, \epsilon\, e^{j\varphi_\ell}} \tag{54}$$

for all φ_ℓ's. Applying (48) – (50) gives the center and radius of the measurement circle in the s^m_{11} plane as

$$s^m_{11\ell} = C_\ell + R_\ell\, e^{j\alpha_\ell} \tag{55}$$

with

$$C_\ell = \frac{a_0 - a_1\, b_1^*\, \epsilon^2}{1 - |b_1|^2\ \epsilon^2} \tag{56a}$$

and

$$R_\ell = \frac{|a_0 b_1 - a_1| \epsilon}{1 - |b_1|^2 \epsilon^2}. \qquad (56b)$$

Again, at least three measurements (three positions of the termination) are required to determine C_ℓ and R_ℓ.

4.2.3. Solution for unknown coefficients

Eqs. (45), (52), and (56) involve the unknown coefficients a_0, a_1, and b_1, the unknown sliding load reflection magnitude ϵ, and the known measurement quantities Γ_s, C_s , R_s , C_ℓ, and R_ℓ. We note that there are eight real equations—two each for the complex-valued equations involving Γ_s, C_s, and C_ℓ, and two real-valued equations involving R_s and R_ℓ. Since there are only seven real unknowns (one for ϵ and two each for a_0, a_1, and b_1), one equation is redundant. The equations used for the solution enforce a) the short to be on the unity circle (an assumed lossless condition), b) the computed reactance circle to be a circle of unity radius centered at zero, and c) the load circle to be centered at zero. These equations may be solved exactly to obtain

$$a_0 = C_\ell C_s / 2 + \Big[R_s^2 - R_\ell^2 - \sqrt{((R_s^2 - R_\ell^2)^2 + (|C_\ell - C_s|^2 - 2 (R_s^2 + R_\ell^2)) |C_\ell - C_s|^2)}\Big] / [2 (C_\ell - C_s)^*], \qquad (57a)$$

$$b_1 = (C_o - a_0) (\Gamma_s - a_0) / (R_o^2 + (\Gamma_s - C_o) (C_o - a_0)) \qquad (57b)$$

and

$$a_1 = - (R_o^2 - C_o (C_o - a_0)) (\Gamma_s - a_0) / (R_o^2 + (\Gamma_s - C_o) (C_o - a_0)) \qquad (57c)$$

with

$$\epsilon = (a_0 b_1 - a_1) R_\ell / ((b_1 C_\ell - a_1)^2 - b_1^2 R_\ell^2). \tag{58}$$

4.2.4. Determining radius and center for the reflection circles

The short and sliding load measurements of the previous sections determine two circles in the complex s_{11} plane,

$$s^m_{11s} = C_s + R_s e^{j\alpha_s}$$

and

$$s^m_{11\ell} = C_\ell + R_\ell e^{j\alpha_\ell}$$

respectively. Here we investigate the mathematics of computing the radii and centers.

Suppose first that we have three measurements s_1, s_2, and s_3, and wish to compute R and C for the circle on which they lie. We begin by drawing two chords joining these points, say chord L_{12} joining s_1 and s_2, and chord L_{23} joining s_2 and s_3. The midpoints of these chords, say p_{12} and p_{23} respectively, are

$$p_{12} = \frac{s_1 + s_2}{2} \quad \text{and} \quad p_{12} = \frac{s_1 + s_2}{2}. \tag{59}$$

The perpendicular bisectors of L_{12} and L_{23} say B_{12} and B_{23} respectively, pass through p_{12} and p_{23} and intersect at the center. We thus need to find the equations of B_{12} and B_{23} to determine where they intersect. These bisectors are given by

$$B_{12} = p_{12} + \alpha_{12}\, j(s_1 - s_2) \tag{60a}$$

and

$$B_{23} = p_{23} + \alpha_{23}\, j(s_2 - s_3) \tag{60b}$$

where α_{12} and α_{23} are real numbers. If we equate B_{12} and B_{23}, the α's may be

determined to give the center C as

$$C = \frac{[s_1(|s_3|^2-|s_2|^2) + s_2(|s_1|^2-|s_3|^2) + s_3(|s_2|^2-|s_1|^2)]}{[s_1^* s_2 - s_1 s_2^* + s_2^* s_3 - s_2 s_3^* + s_3^* s_1 - s_3 s_1^*]}. \tag{61}$$

The radius is then given by $|s_1 - C|$. The best numerical conditioning results when the three points s_1, s_2, and s_3 are nearly equally–spaced around the circumference of the circle. This conclusion is true for two reasons: 1) with (s_1-s_2) or (s_2-s_3) small, the denominator of (61) becomes small, leading to possible roundoff error. 2) with (s_1-s_2) or (s_2-s_3) small, R and C become very sensitive to small errors in the measurements (due, for example, to noise in the system).

If the measurements s_i are noisy, or are suspect for any reason such as lossy connectors, it is preferable to use more than three points to define the circles. In this case, a best–fit procedure, rather than Eq. (61), is needed. One possible best–fit approach is described in the next section.

4.2.5. Least–squares circle fitting

Our problem is to find the circle that "best" fits a collection of measurements $\{s_i \mid 1 \le i \le k, k > 3\}$, in some sense of the word "best." A common measure of the goodness of fit, and the one that will be employed here, is least squares (the curve, in this case the circle, is chosen to minimize the mean square error in radius over the data points).

Once again, the measured points in the complex s_{11} plane will be denoted $s_1, s_2, \ldots, s_n$. The desired representation is a circle

$$s_{11} = C + R\, e^{j\varphi}. \tag{62}$$

The error between measured point s_i and the best–fit circle is

$$\epsilon_i = |(|s_i - C|) - R|. \tag{63}$$

Possible phase errors in s_i (that is, errors that displace s_i around the circle but not away from it) do not influence the best–fit choice of C and R. Thus the least–squares problem reduces to that of choosing C and R for minimum error.

Using the error representation of (63), the mean square error is given by

$$F(C,R) = \textit{mean square error} = \sum_{i=1}^{N} (|s_i - C| - R)^2. \tag{64}$$

To determine the minimum of F, we differentiate with respect to R, $Re(C)$, and $Im(C)$ and set each derivative to zero. Thus we have

$$\frac{\partial F}{\partial R} = -2 \sum_{i=1}^{N} (|s_i - C| - R) = 0 \tag{65a}$$

$$\frac{\partial F}{\partial Re(C)} = 2 \sum_{i=1}^{N} (|s_i - C| - R) \frac{Re(C - S_i)}{|C - s_i|} = 0 \tag{65b}$$

and

$$\frac{\partial F}{\partial Im(C)} = -2 \sum_{i=1}^{N} (|s_i - C| - R) \frac{Im(C - s_i)}{|C - s_i|} = 0. \tag{65c}$$

Eq. (65a) is easily solved for R to obtain

$$R = \frac{1}{N} \sum_{i=1}^{N} |s_i - C|, \tag{66a}$$

while Eqs. (65b) and (65c) may be combined to obtain the function

$$f = C - \frac{1}{N} \sum_{i=1}^{N} (s_i + R \frac{C - s_i}{|C - s_i|}) = 0. \tag{66b}$$

In general, (66) must be solved iteratively. We have implemented a secant optimization routine which performs well for most cases of interest. On occasions, the center will tend to infinity, which also offers a zero to f. This tendency is associated with clustering of the data points with a related inability to fit a circle

properly. This problem specifically occurs at 10.7 GHz for the sliding load used in the HP system with the spacings designated on the sliding load body. Even HP recommends additional sliding load data points to alleviate this problem.

To help avoid the potential infinities, F was modified to include an additional R^2 multiplier as

$$F = \sum_{i=1}^{N} (|s_i - C| - R)^2 R^2. \tag{67}$$

To simplify the process, R was taken to satisfy (66a) rather than the new equation obtained by differentiating F with respect to R. This choice gives an optimizing function of the form

$$f = [C - \frac{1}{N} \sum_{i=1}^{N} (s_i + R \frac{C - s_i}{|C - s_i|})] R^2$$

$$+ 2 R \frac{1}{N^2} \sum_{i=1}^{N} (|s_i - C| - R)^2 \sum_{i=1}^{N} (\frac{C - s_i}{|C - s_i|}) = 0. \tag{68}$$

Again, (68) is solved iteratively for C using (66a) to define R. This equation has resulted in excellent results for the computed circles. Hewlett–Packard has suggested a modified procedure for finding the circles which minimizes the mean–squared error of the squared radius. A definite advantage of this procedure is the existence of a closed–form solution requiring no iteration. This approach has been modified to include the reactance circle form to be presented in Sec. 4.2.6. The resulting equations have been implemented for the calibration process and has been found to give excellent results. An alternate form has been developed which minimizes the least square error of the center from the bisectors of all point sets. This latter technique may be solved in closed form and gives excellent results as shown in Fig. 4 for the phase of the HP "open". The figure also includes the

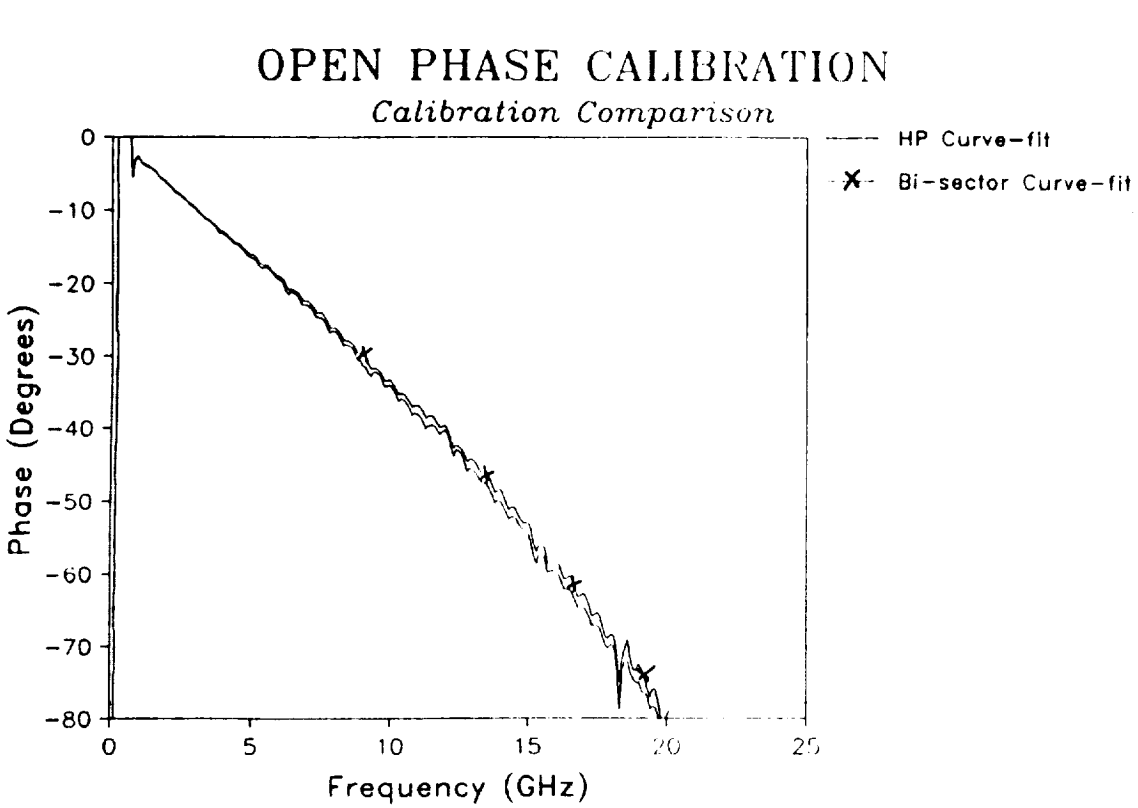

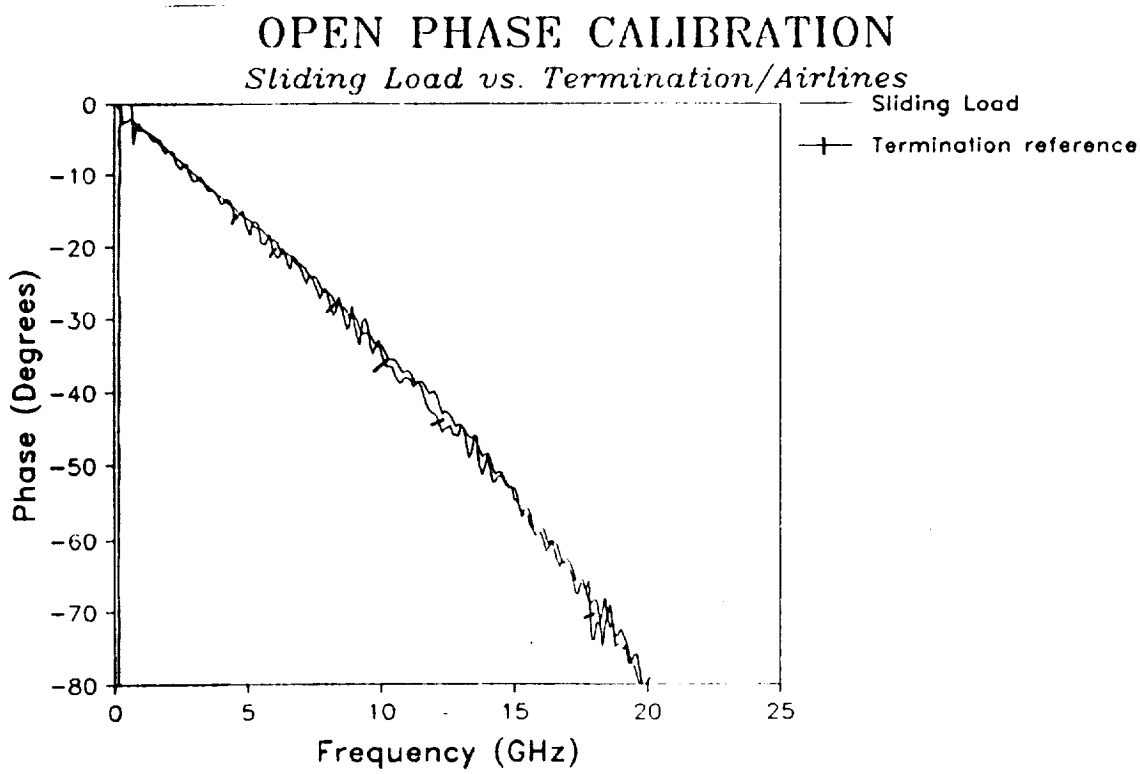

Figure 4. a) Calibration of the HP "open" phase based on the modified HP circle fitting procedure and the bisector form. b) The effects of the sliding load and a fixed load on varied line lengths are also shown.

effects of using the sliding load versus fixed terminations mounted on the ends of airlines, to be discussed in more detail in the next chapter. The modified HP form is currently being used for the curve–fit procedure.

4.2.6 Center and radius of reactance circles

The reactance circles provide for a modification in the circle fitting procedure. First, we assume that the short is ideal and the circle must go through this point. As a result it is simple to estimate the radius as

$$R = |s_1 - C|. \tag{69}$$

In addition, we assume that the "open" is an ideal reactance. In other words, it has a reflection coefficient of unity magnitude. Thus the center of the reactance circle must lie on the curve defined by

$$C = \frac{(s_1 + s_2)}{2} + j\, x\, (s_1 - s_2) \tag{70}$$

with x the only unknown.

If we now differentiate (67), after the substitution of (69) and (70), with respect to x and set the result to zero we obtain

$$f = \frac{\partial F}{\partial x} = 2 R^2 \sum_n \left\{ \left(1 - \frac{R}{|s_n - C|}\right) Re[(C - s_n)\ (j\ (s_1 - s_2))^*] + [(1 - \frac{|s_n - C|}{R})^2 + (1 - \frac{|s_n - C|}{R})]\ |s_1 - s_2|^2\ x \right\} = 0. \tag{71}$$

With this form, the algorithm uses a short circuit reference, and a collection of additional reactance references (not necessarily of known reactance). The open circuit is used as a preferred first unknown reactance on which the line defining the circle center is based. This is primarily used due to the probability of additional loss in the other references. The remaining reactances are obtained by using several airlines,

preferably with nonharmonic related lengths, terminated in both a short circuit and an open circuit. The used of both the short and open is to counteract the errors in the circle determination arising due to loss in the airlines. The short and open combinations tend to average out the loss effect by appearing on opposite sides of the reflection coefficient plane. As with the load curve–fit, the reactance circle routine has been modified to use both the bisector and the HP approaches rather than the minimization of (67). These approaches have given improved results and the modified HP form is currently in use.

Detailed discussions of the calibration process and the measurements of component standards are provided in the next chapter. In addition, models are developed for the actual open circuit references and terminations. Consideration is also given to the possible imperfections in the short circuit reference.

CHAPTER 5
RESULTS OF REFLECTION MEASUREMENTS

This chapter presents the results of the calibration procedures developed in the previous chapter for reflection measurement. This procedure requires no source or test port switching and thus does not have any errors associated with such switching. The errors which occur are thus fundamental errors in calibration or system errors associated with the network analyzer sweep circuits, frequency sweep, or discretization. The data was taken on an HP 8510 network analyzer system with an Hp 85080A, 7mm, calibration kit. Initially, we will consider the basic measurement and associated calibration. We will then consider the modeling of both the "open" standard and the fixed termination.

5.1 Basic Measurement and Calibration

In the HP system, two termination standards are provided for use. An excellent fixed termination is provided for use below 2 GHz and a sliding load is provided for use above 2 GHz. To avoid problems with imperfections in the fixed termination, it was used at the end of a series of 50 ohm, beaded, precision airlines to provide a load circle similar to the sliding load. This approach to the termination problem gives good results over the entire frequency range as shown in Figure 5. However, the fixed load does have an oscillatory error. In the realm above 2.0 GHz, the sliding load provides excellent results. In fact, the sliding load

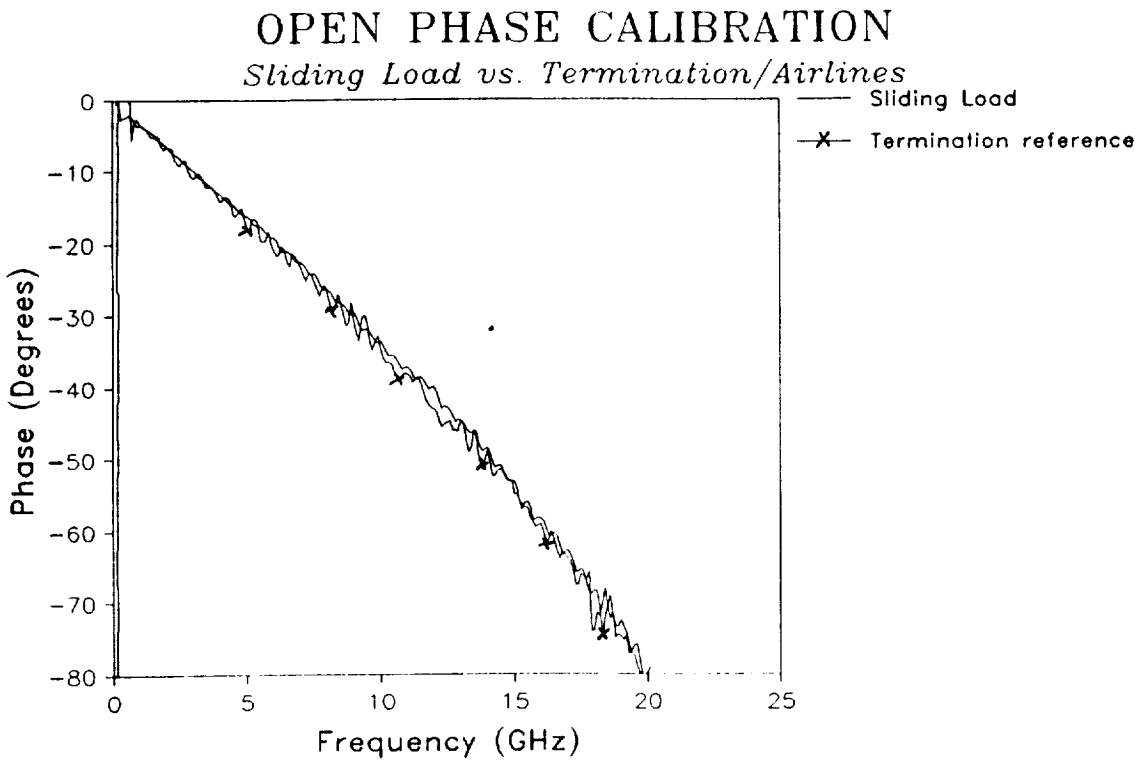

Figure 5. Comparison of the calibration for the HP open phase using a fixed termination terminating airlines and using a sliding load.

works well down to 0.5 GHz. The reactance calibration was obtained with both short and open references and both the short and open terminating the same airlines. The open was treated only as an unknown reactance while the short was considered perfect. The data calibration is an improvement over the simple calibration using the termination references, the HP open, and a short. The full calibration required the determination of circles which best fit the calibration data discussed in Chapter 4.

5.2 Modeling the Open Calibration Standard

To address the full calibration process, we are interested in determining a model for the HP open. We have three different models for the open as a frequency dependent capacitor readily available. A modified form of the 2–term data for the Hp open #2 is provided by Innovative Software. This model is a two term power series given by

$$C = 0.0905 + 0.0000785\, f^2 \quad \text{pF} \tag{72}$$

for f in GHz, with a phase error for the resultant phase calibration as shown in Figure 6. As in all the plots to follow, the calibration has been done using the short reference, airlines terminated in both a short and a open for the reactance circles, and either the sliding load or a fixed termination on a series of airlines for the 50 ohm reference. The estimated phase in Figure 6 was determined by using the C of (72) to model the open.

Similar results are shown in Figures 7 and 8 for three and four term power series approximations to the capacitance given by Hewlett–Packard. These series are respectively

$$C = 0.09285 + 0.0000072\, f^2 + 0.0000043\, f^3 \quad \text{pF} \tag{73}$$

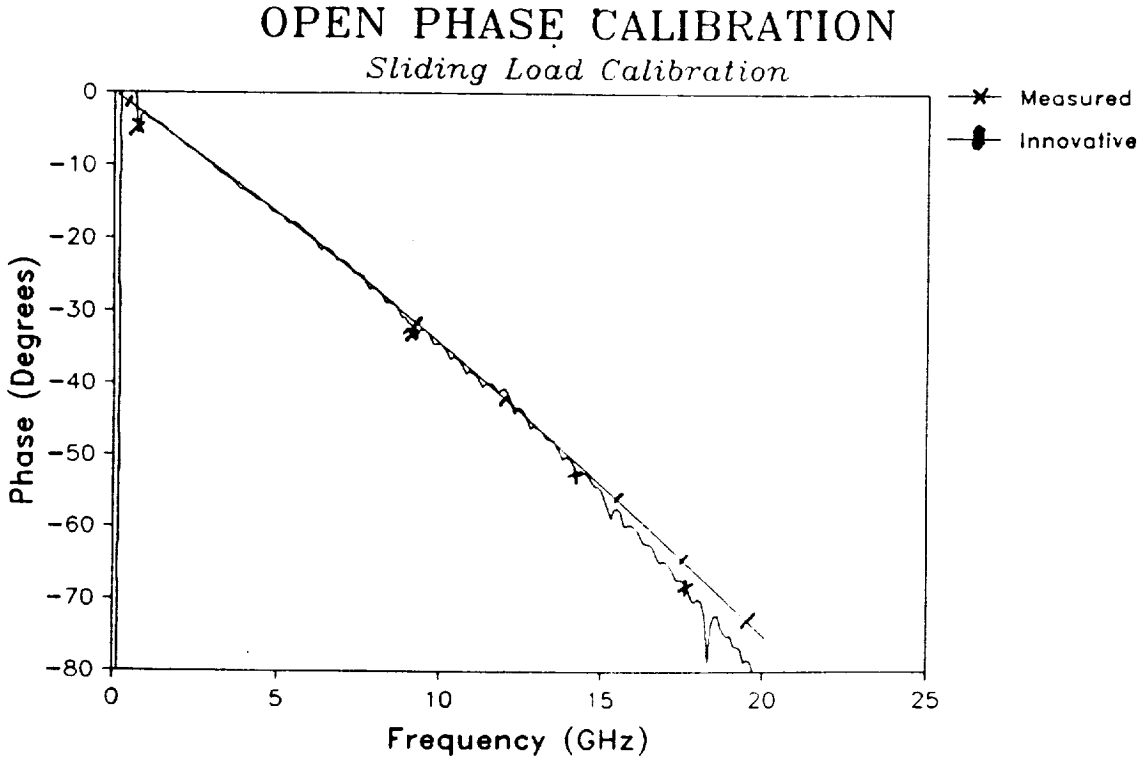

Figure 6. Comparison of the calibration for the HP open phase to the phase based on the two–term capacitance model of IS.

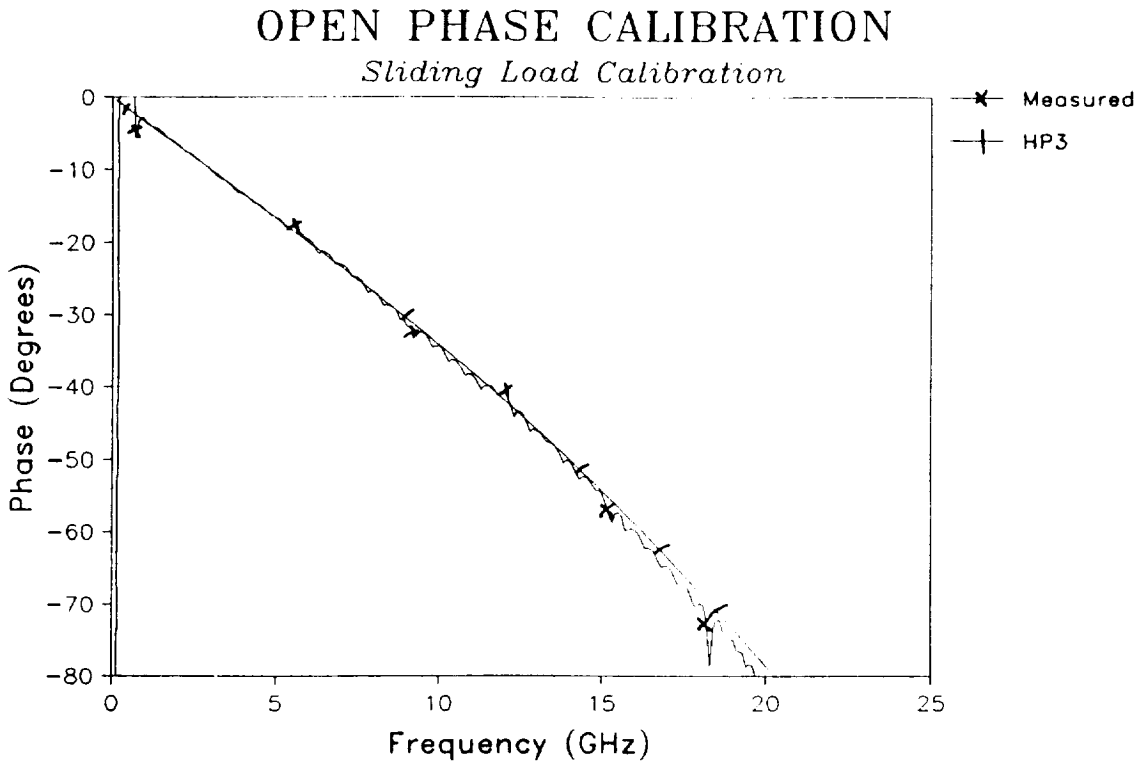

Figure 7. Comparison of the calibration for the HP open phase to the phase based on the three–term capacitance model of HP.

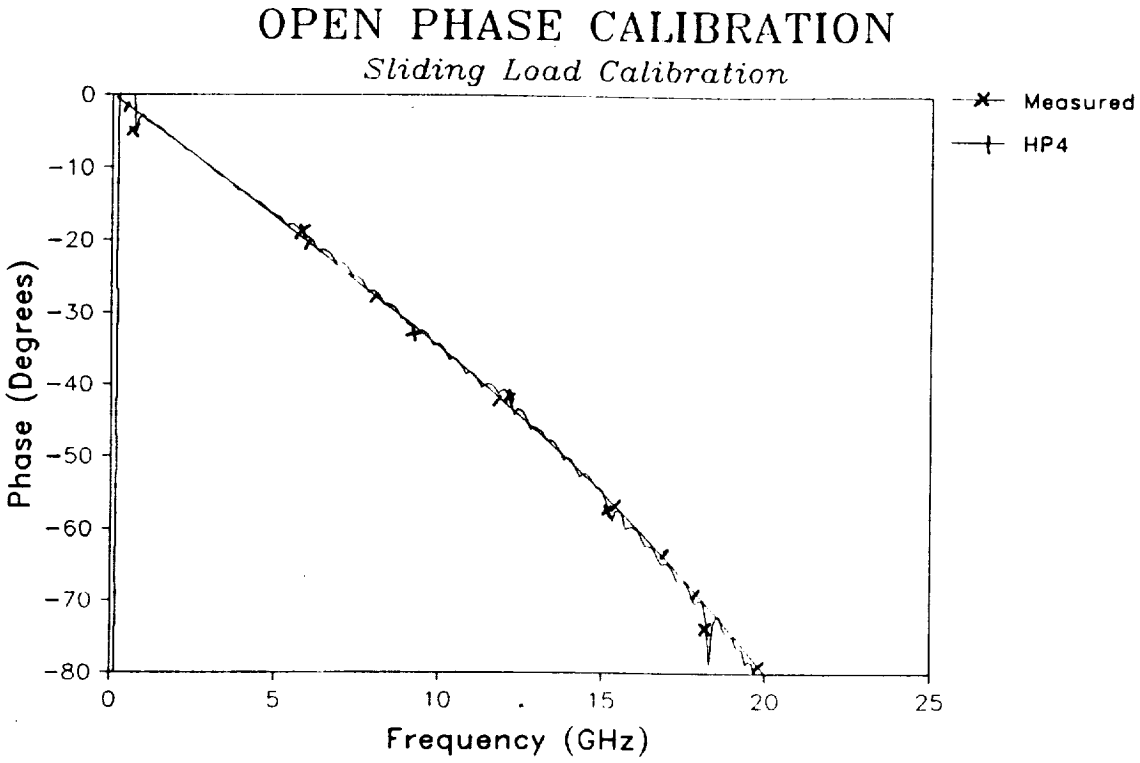

Figure 8. Comparison of the calibration for the HP open phase to the phase based on the 4–term capacitance model of HP.

and

$$C = 0.0872 + 0.001695\, f - 0.00015\, f^2 + 0.0000089\, f^3 \text{ pF} . \quad (74)$$

The initial goal of this work has been to develop a model for the capacitor. This improved model may then be used for future calibration. The process used to calibrate the open may also be used in situations when the open may not be used directly. To model the open, the calibrated phase (or effective capacitance) was fit to a corresponding model of the open. This curve fit was forced to minimize the phase errors between the measured data and the model. Four basic models were chosen for consideration: a two term series like (72); a three term series like (73); a three term series (denoted formula) with the series forced to the capacitance of the HP three term series at 40 GHz; and an inductor in series with a capacitor to represent the delay inherent in the open circuit connection. The results are indistinguishable in plot form as shown in Figure 9 for the inductive expansion and the first 3–term series.

To obtain the results of Figure 9, the phase of the open reference was matched to that of the model used for the open. The results for the inductive termination model are shown in Figure 10. This model shows an improvement over the fits of the HP 3–term model and the Innovative Solutions model shown in Figures 6–7. A similar improvement is also found if the calibrated capacitance of the open is compared to the estimates based on the other two circuit models. Figures 11 and 12 depict the calibrated capacitance using the reactance circle approach as compared to the HP 3–term model and the inductive model. In particular, the capacitance is over estimated for the HP model. The low frequency error arises due to the inability to fit a circle to the load points adequately.

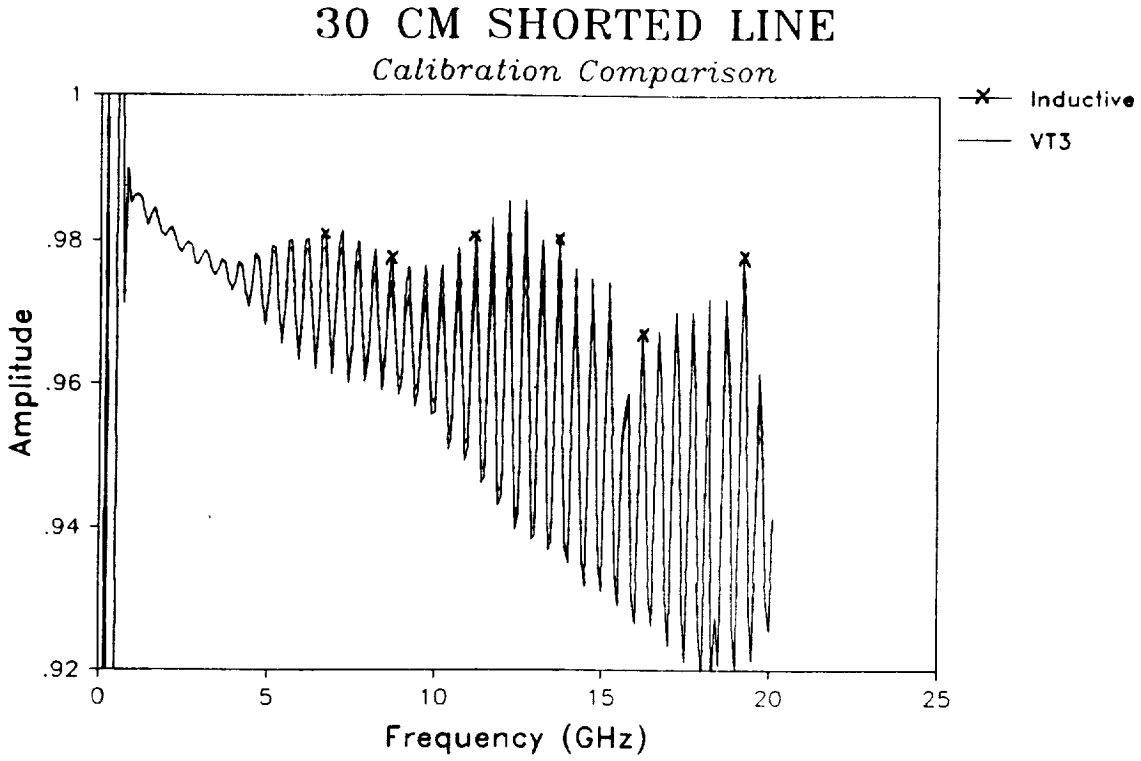

Figure 9. Comparison of the calibrated amplitude of a 30 cm airline using both the inductive and 3–term capacitive models of Virginia Tech.

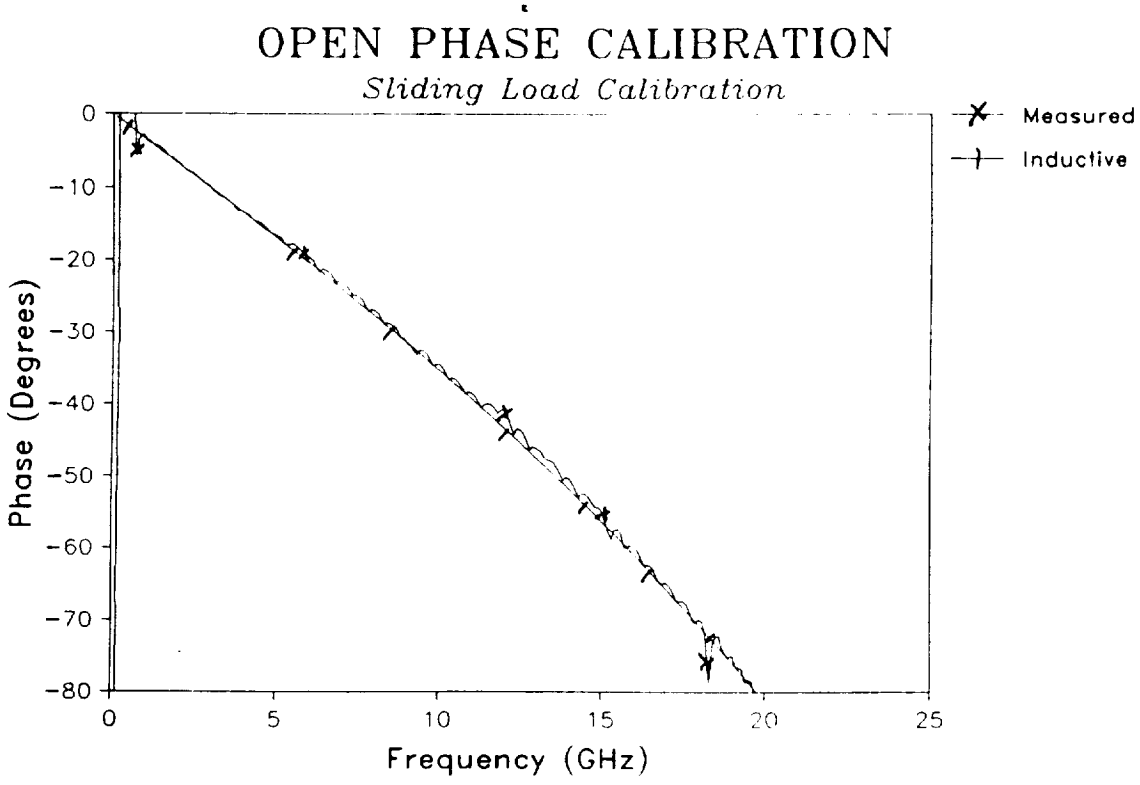

Figure 10. Comparison of the calibration of the HP open phase to the phase based on the Virginia Tech inductive model.

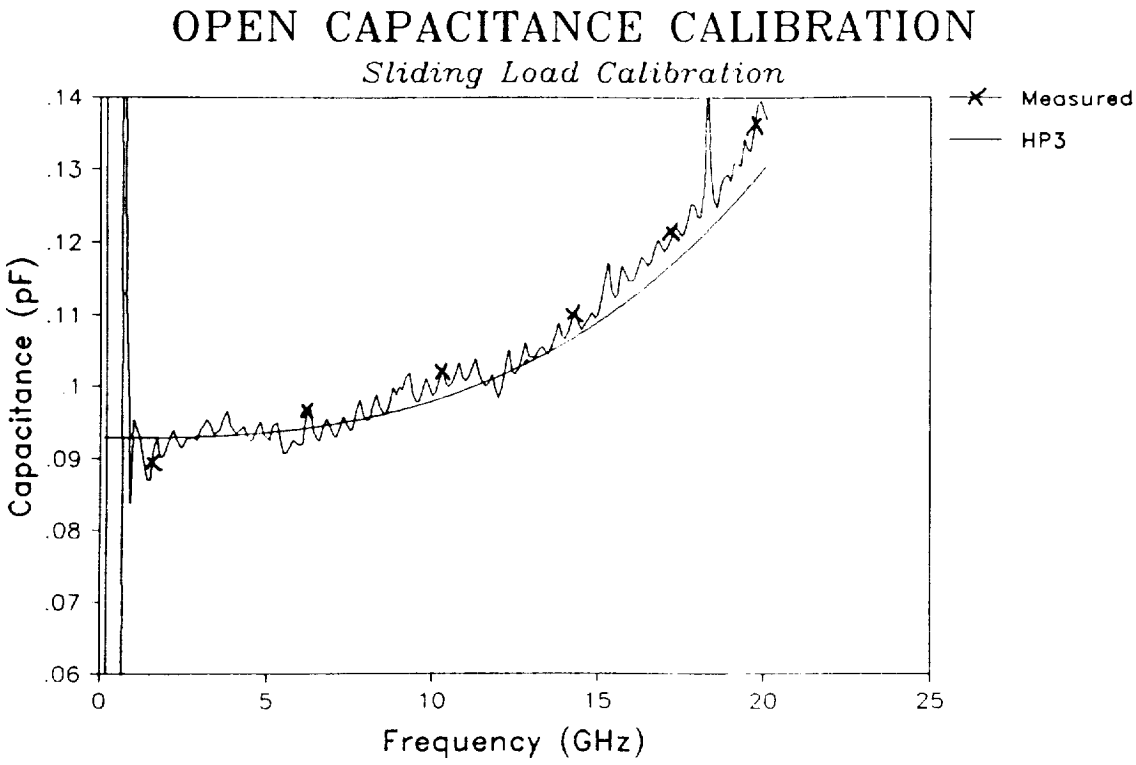

Figure 11. Comparison of the calibrated capacitance of the HP open and the HP 3–term series model.

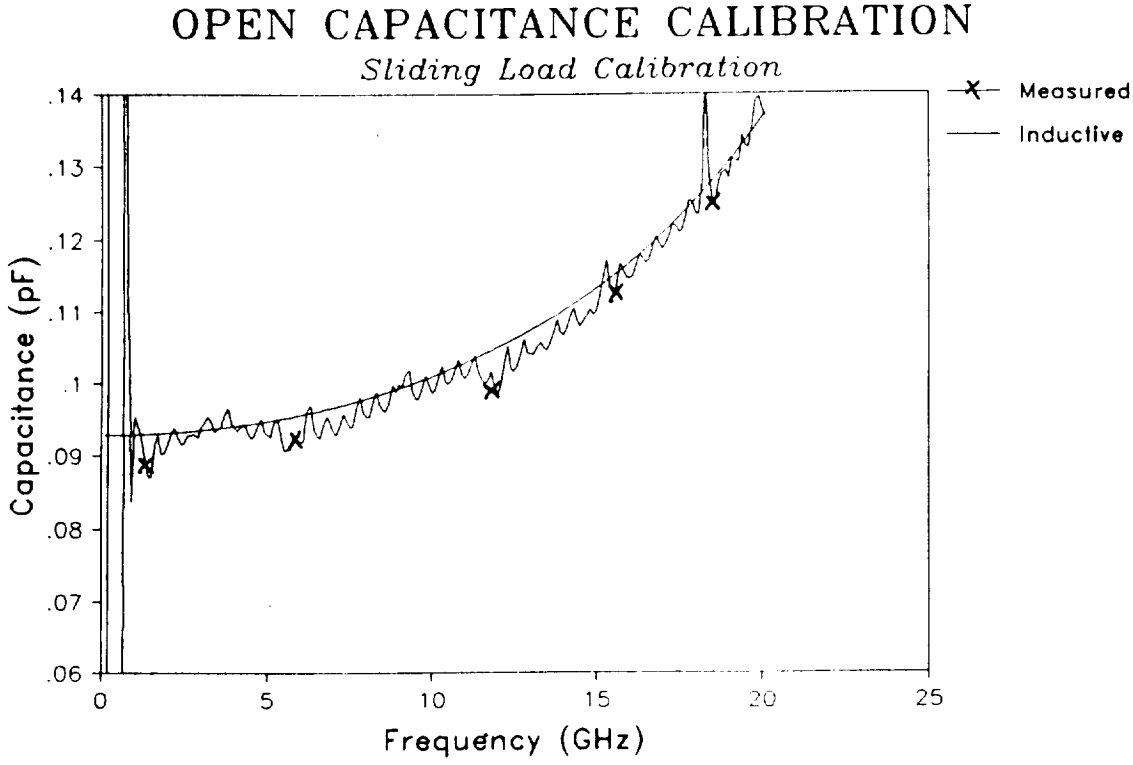

Figure 12. Comparison of the calibrated capacitance of the HP open and the Virginia Tech inductive model.

The importance of the calibration standard modeling is emphasized in a plot of the reflection coefficient of a 30 cm shorted airline. This is the classic problem which has made researchers suspicious of the HP calibration system. If the standard models are in error, the response for the 30 cm airline shows an oscillatory behavior which may even give the false concept of an airline with power gain. Such data is presented in Figures 13 through 17 using data collected on an HP 8510 computer–based network analyzer system.[4] The HP 3–term and 4–term series are out of phase with those of the Innovative Software data at the high frequency end and represents an apparent underestimating of the capacitance of the open standard for the Innovative Software data. The Virginia Tech calibrations using a 3–term series and an inductive model both fit the data with large excursions. Though there was and excellent fit to the open data, there appears to be an error in the Virginia Tech capacitance estimate of the open. However, this data was taken for a 30 cm beaded airline which may have some resonances due to the beads. To check our results, we should view the 30 cm line terminated in a short circuit using the sliding load data of Fig. 18. This data used the collection of airlines for calibration rather than the open model. This data is compared with the 3–term VA Tech model and the 4–term HP model in Figs. 19 and 20 respectively.

5.3 Modeling the Fixed Termination Standard

In many instances, we would expect the calibration effects of the termination reference also to become important. To develop a model for the termination, we may consider the amplitude and phase plots of Figure 21. Though there is a fair amount of noise on the data due to the resolution which is approaching the discretization of the system used, it is apparent that the termination may be modeled

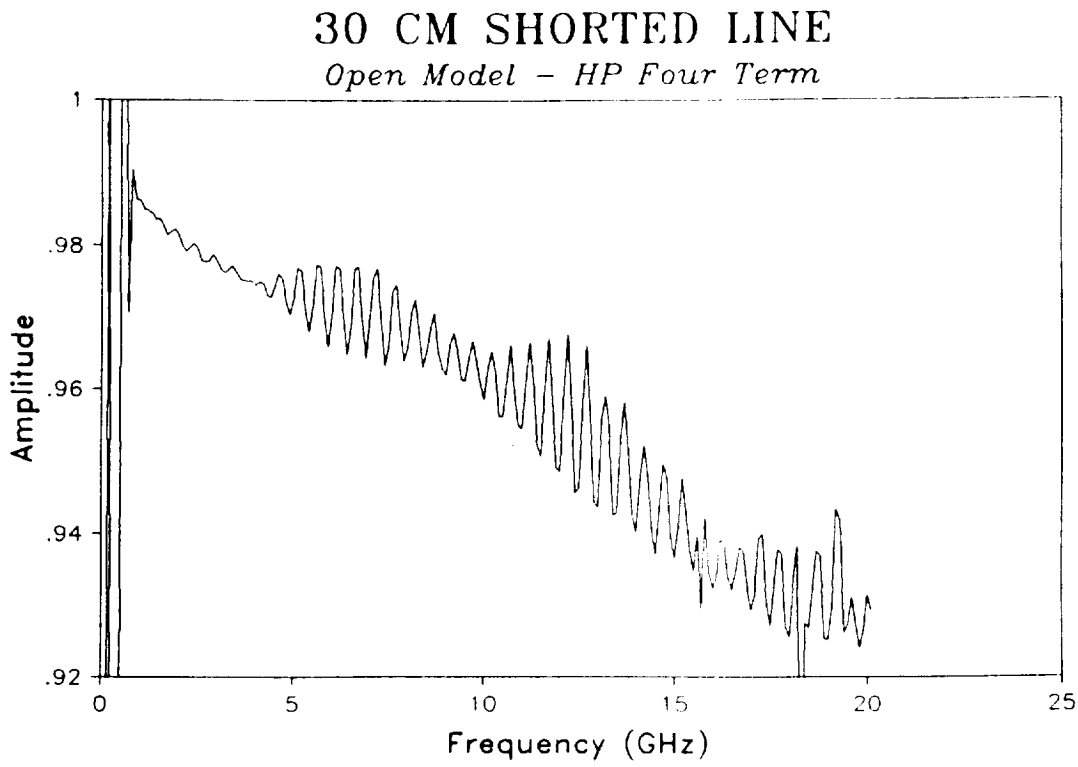

Figure 13. Calibration of a 30 cm beaded airline using the HP 4–term capacitance model.

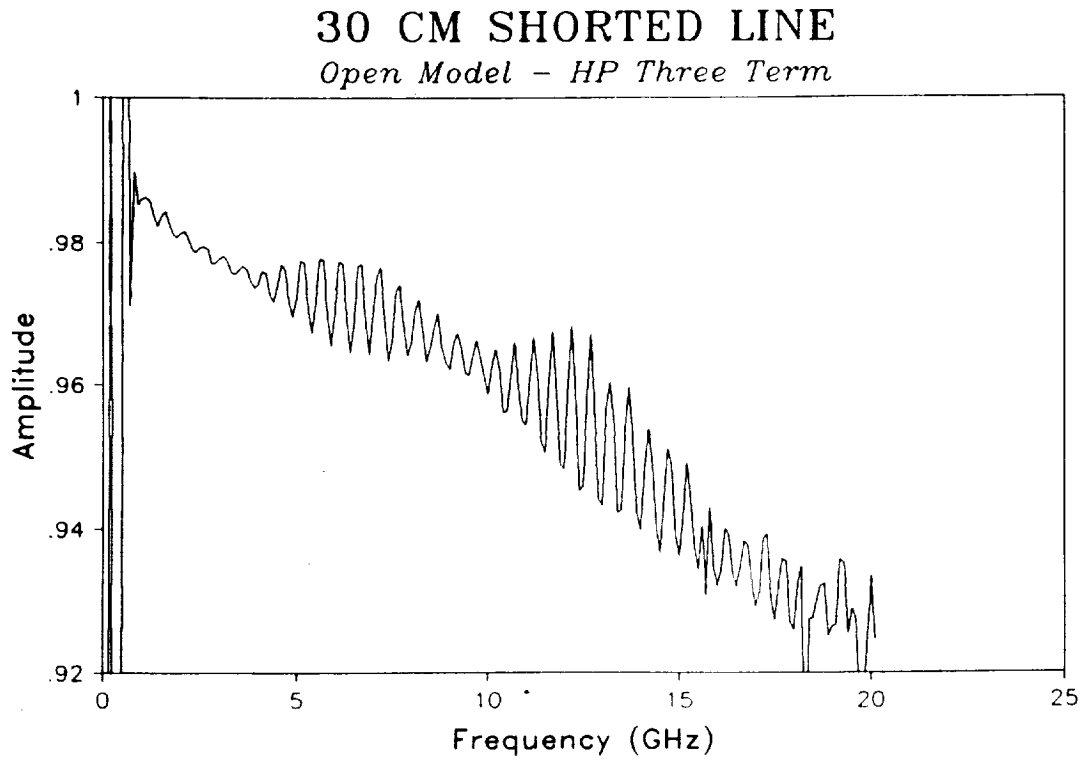

Figure 14. Calibration of a 30 cm beaded airline using the HP 3–term capacitance model.

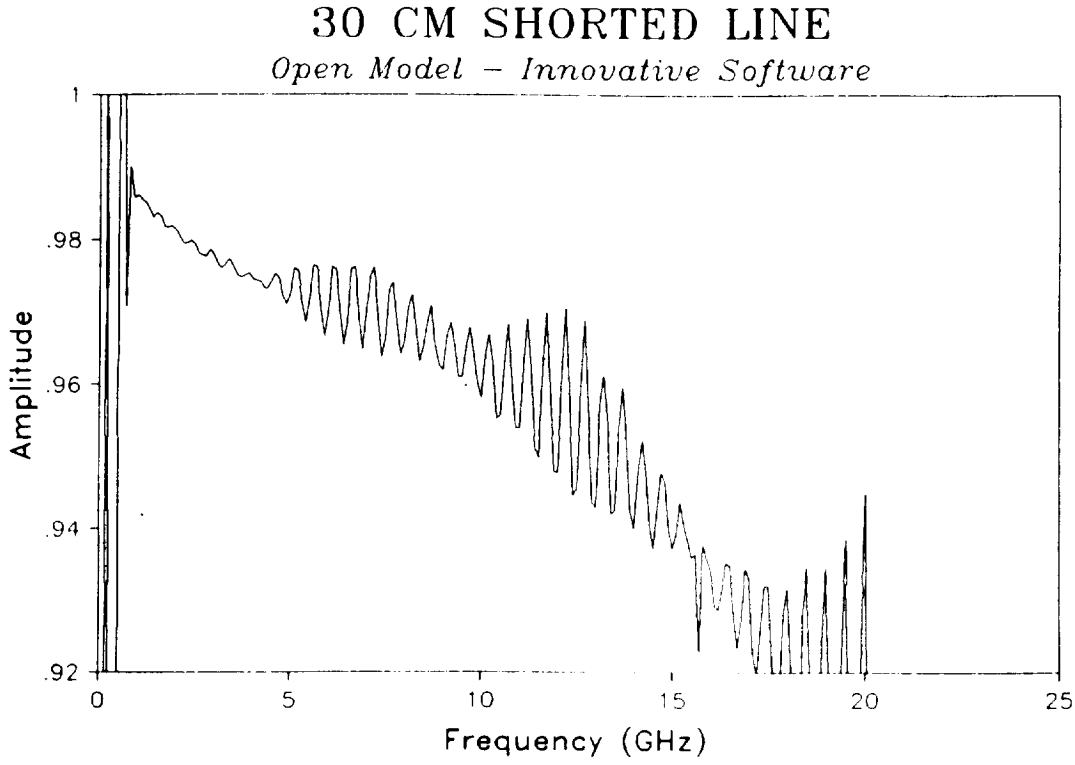

Figure 15. Calibration of a 30 cm beaded airline using the Innovative Software capacitance model.

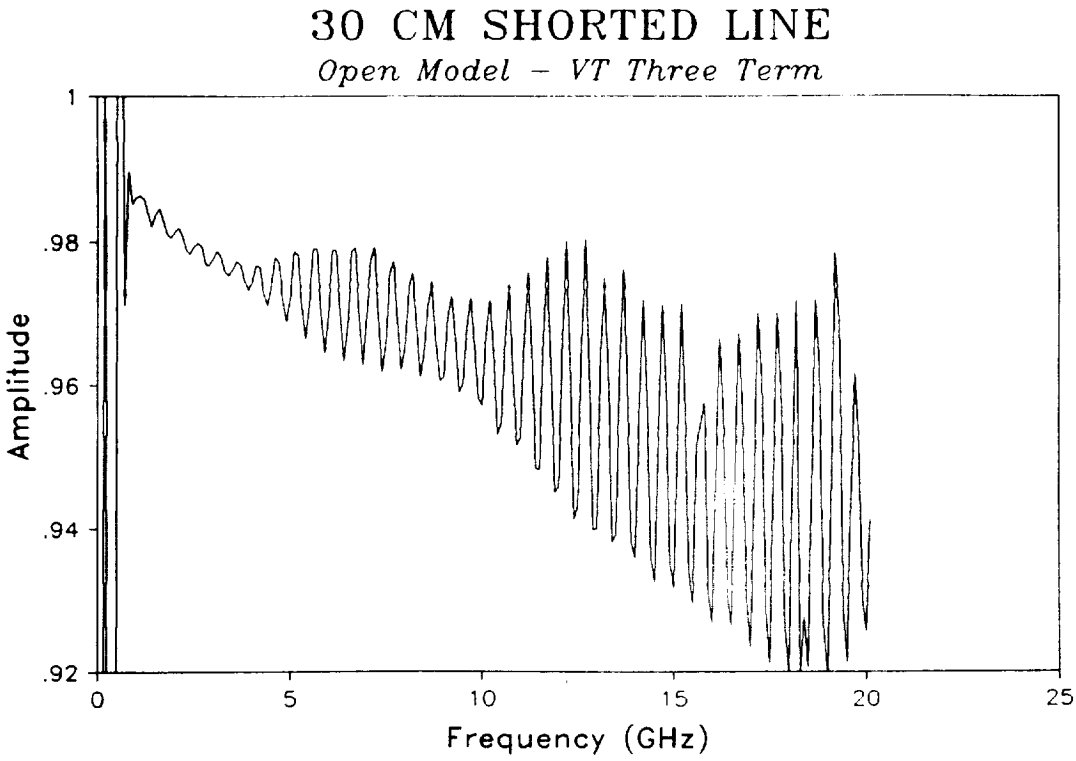

Figure 16. Calibration of a 30 cm beaded airline using the Virginia Tech 3–term capacitance model.

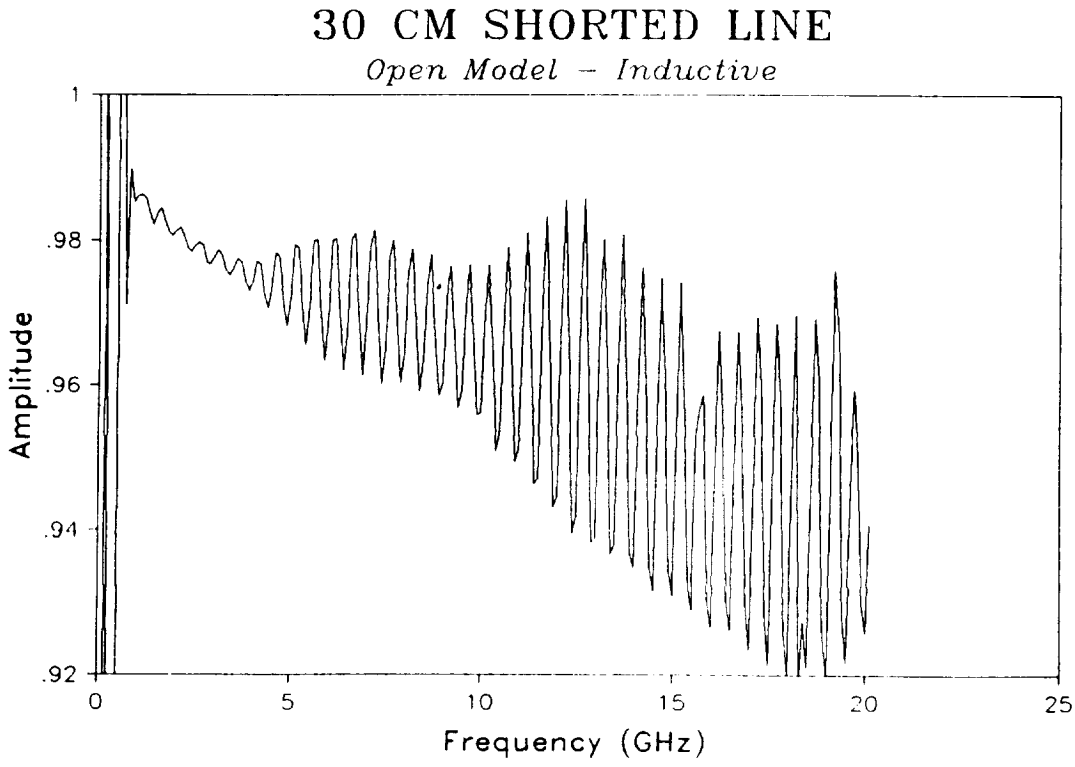

Figure 17. Calibration of a 30 cm beaded airline using the Virginia Tech inductive model.

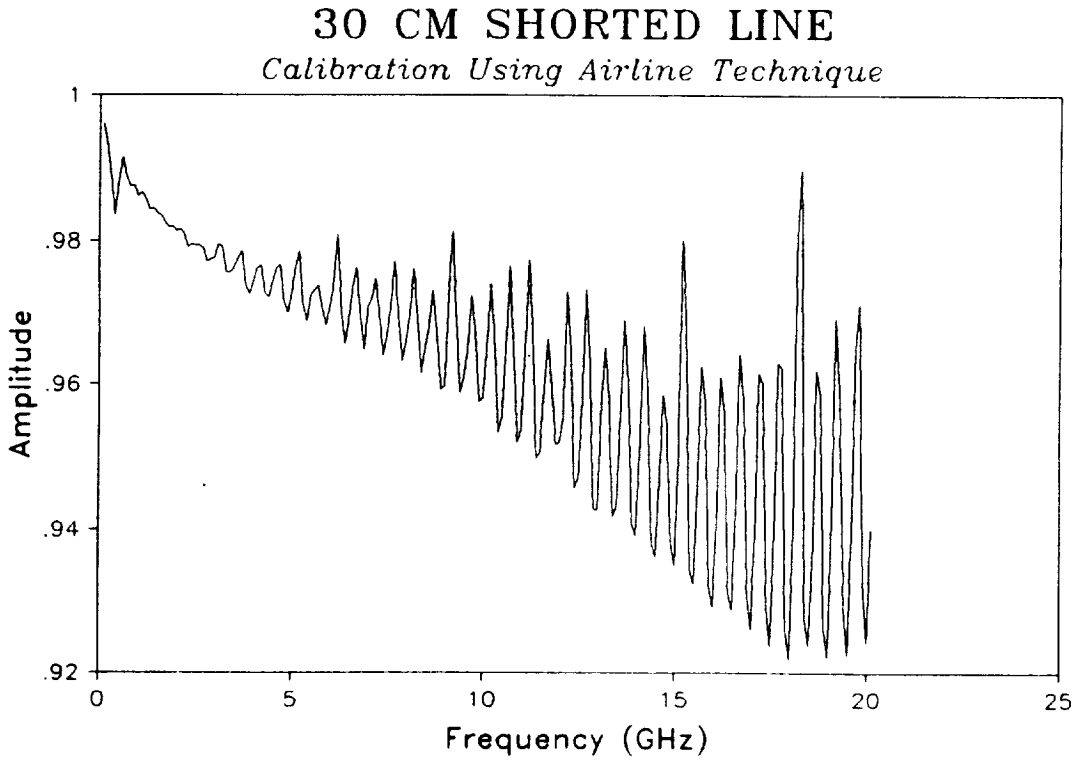

Figure 18. Calibration of a 30 cm beaded airline on a HP 8510 using the multiple airline calibration technique.

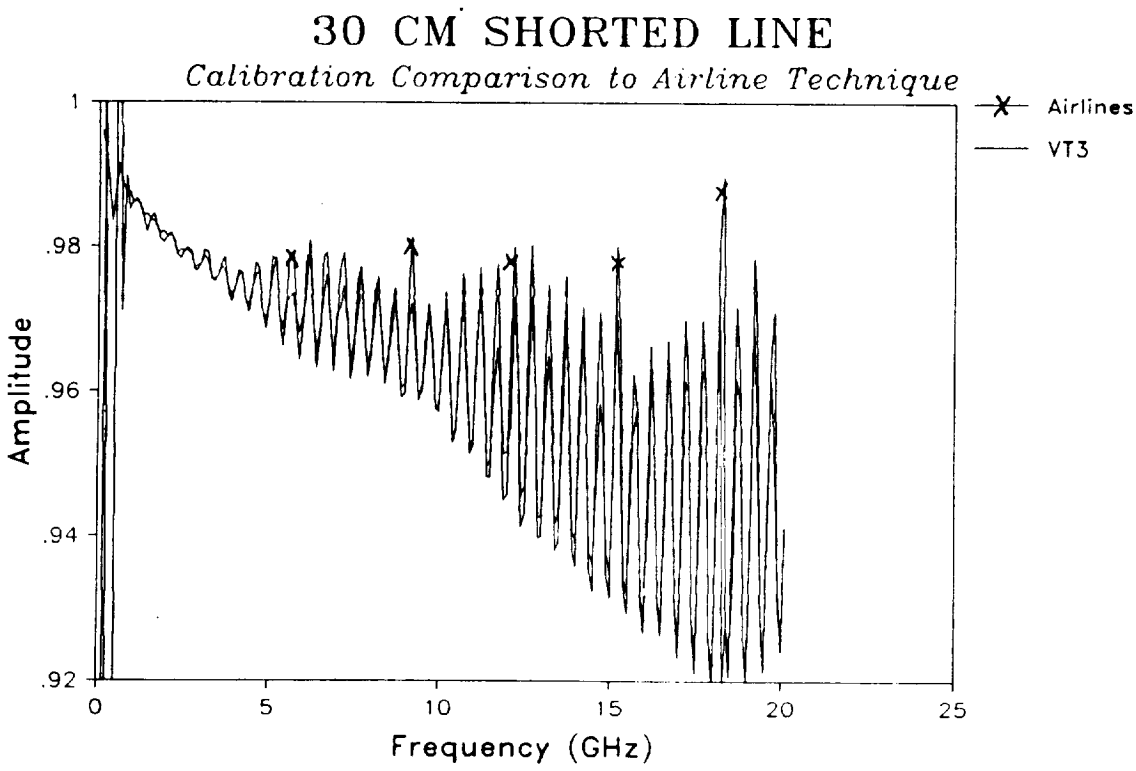

Figure 19. Calibration of a 30 cm beaded airline on a HP 8510 using the VT 3–term capacitance model and the airline technique.

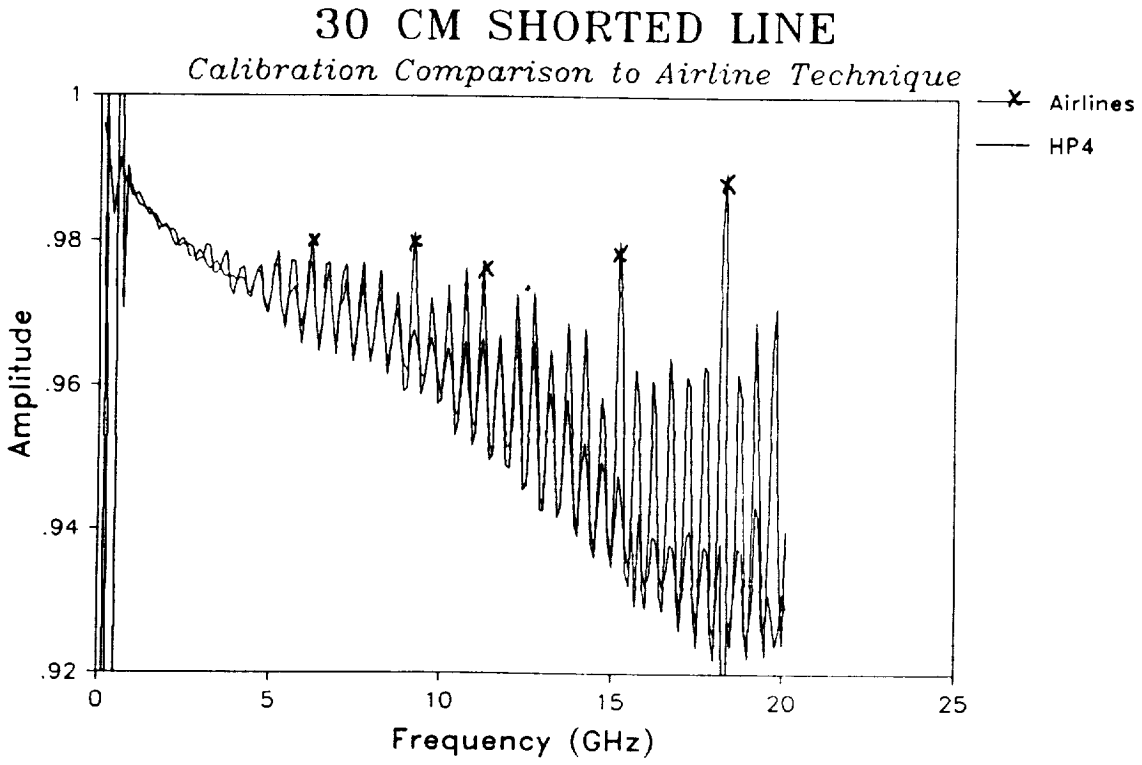

Figure 20. Calibration of a 30 cm beadless airline on a HP 8510 using the HP 4–term capacitance model and the airline technique.

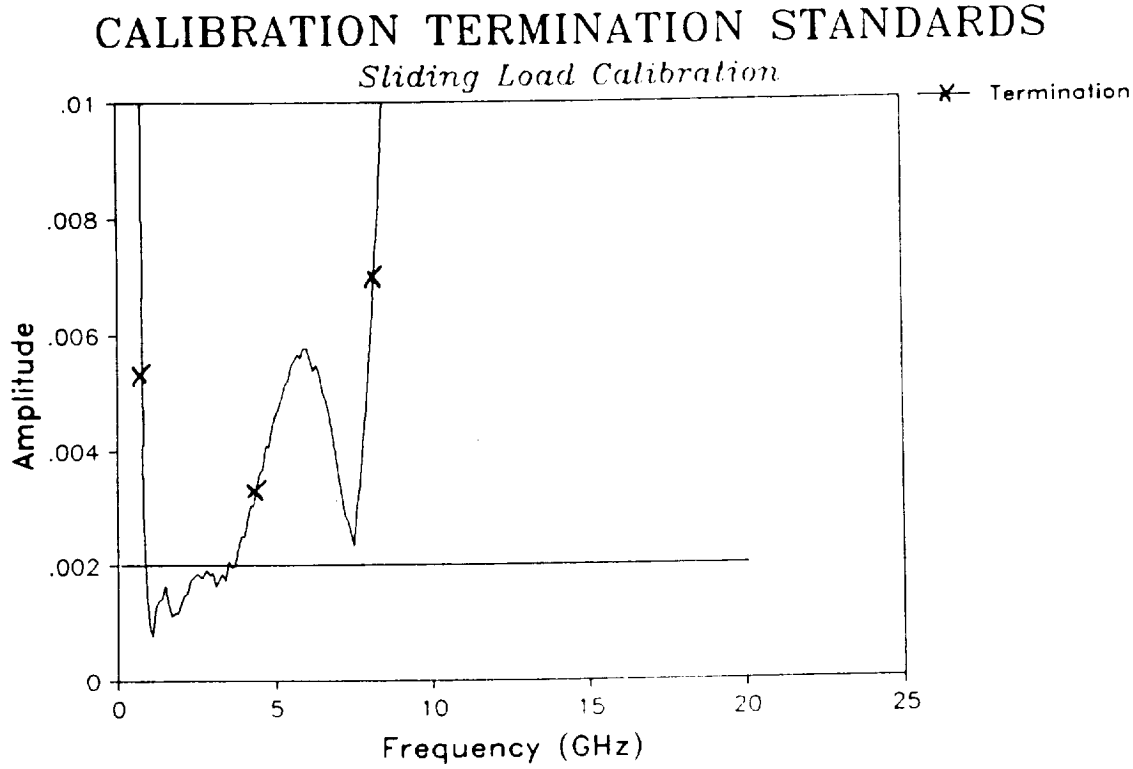

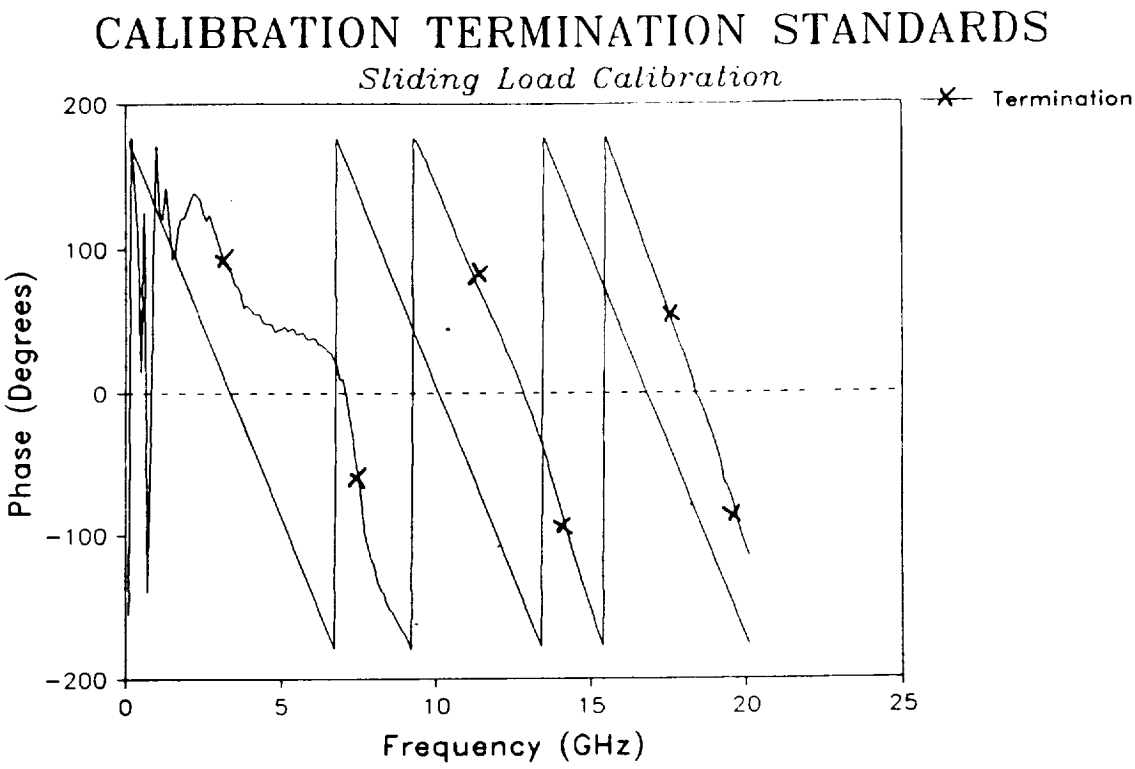

Figure 21. Calibration of the fixed termination using the inductive model for the open and the fixed termination with several airlines to define a load circle.

reasonably well by a fixed resistor at the end of a length of line. The actual length is difficult to estimate, though it appears to be between 3 to 4 cm. A description of the actual termination is shown in Figure 22, with the appearance of a thin film resistor 0.8785 inches from the connector face. Using a HP 4192A low frequency impedance analyzer at 1000 Hz, the resistance is found to be 49.30 ohms at -0.12°. This measurement gives a reflection coefficient of –0.007 which differs from the –0.002 reflection coefficient below 2 GHz of Fig. 22a, though within reasonable limits in absolute resistance. This latter corresponds to 49.9 ohms at low frequencies. If we estimate the length to the resistance to be the 0.8785 in distance to the connector face, the one half to account for its distributed nature, we obtain an effective length of 2.231 cm. The data for 49.8 ohms located 2.231 cm from the connector face has been plotted in Figure 21. The result is about twice that needed to fit the data. The error results from the capacitive washer which effectively shortens the line.

The effect of this termination model is not always critical as is seen in the reflection amplitude of the open standard. These results shown in Fig. 23 were obtained assuming the termination was a perfect 50 ohm termination. The calibration of the open circuit reference using the 50 ohm assumption has excellent results below about 5 GHz.

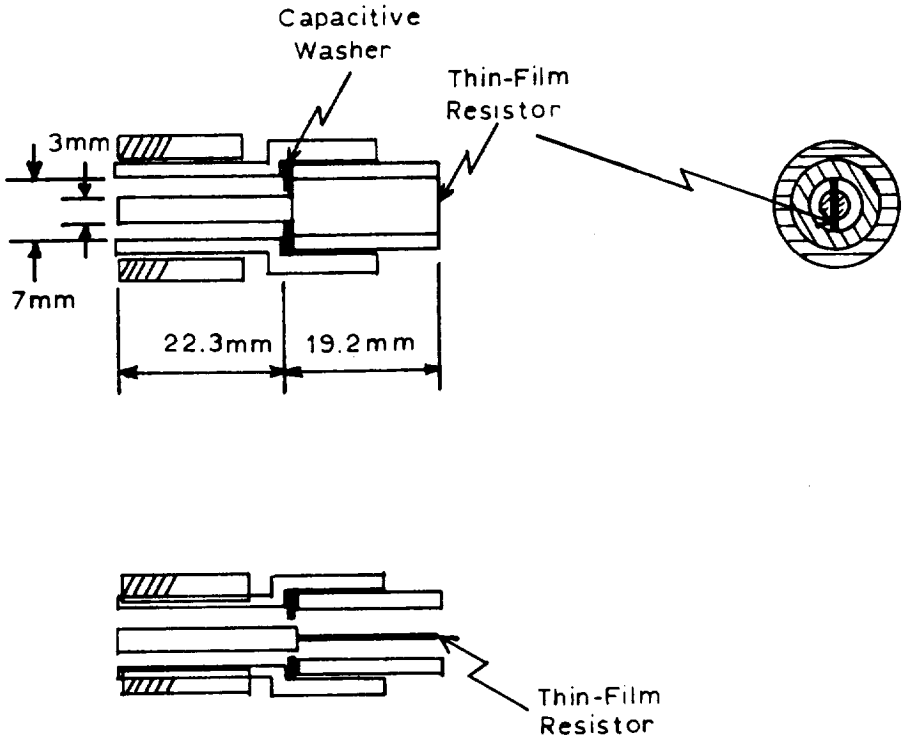

Figure 22. Construction details of the HP fixed termination standard.

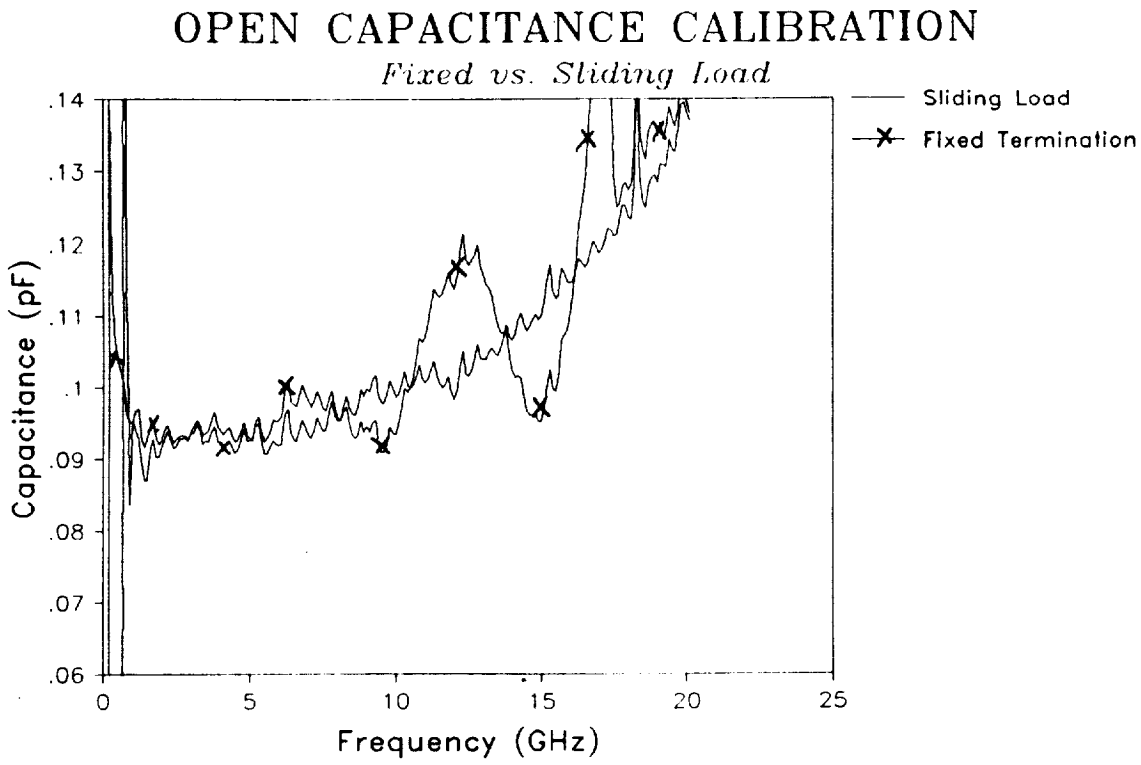

Figure 23. Calibration of the 30 cm beaded airline using a) the fixed termination on a series of airlines and b) the fixed termination exclusively as a 50 ohm standard below 2 GHz.

5.4 The Effect of a Nonideal Short Circuit Reference

Before we complete this chapter, we should consider the last calibration assumption used in commercial systems in addition to the calibration steps above. If you have not already considered the possibility, the short circuit standard does not necessarily have a reflection magnitude of unity. We now address this last concern, but we will not complete the implementation necessary to incorporate the nonideal short effect into the calibration in this report.

We assume that the electromagnetic fields in the vicinity of the short circuit reference form a TEM mode in the transmission line. At the short we will determine the relection in a planewave sense from a conducting wall with a finite conductivity. In the planewave problem, the characteristic impedance of copper is

$$\eta_c = \sqrt{\frac{j\omega\mu}{\sigma + j\omega\epsilon}} . \tag{75}$$

For copper μ is $4\pi \times 10^{-7}$ H/m, ϵ is approximately $\frac{1}{36\pi} \times 10^{-9}$ F/m, and σ is 5.8×10^{7} S/m. Determining the reflection coefficient of η_c with respect to η_0 for free space we obtain

$$\Gamma_s = \frac{\sqrt{j\omega\epsilon} - \sqrt{\sigma + j\omega\epsilon}}{\sqrt{j\omega\epsilon} + \sqrt{\sigma + j\omega\epsilon}} \tag{76}$$

which at 10 GHz is $(0.99986 \angle 179.99^\circ)$. At 40 GHz this becomes $(0.99945 \angle 179.97^\circ)$. Thus we find that the effect of the loss in a copper short circuit standard should only cause a variation on the order of 0.05 %. If the system is to be taken to the limit for a precision of 0.01%, then this correction would become critical. In the applications for which systems are currently used, this correction is not necessary and is not considered further here.

We have seen in this chapter, the importance of proper modeling of the standards used in the calibration of a network analyzer system. If such corrections

are not used, the resultant data can not attain the accuracy limits of the system in use. This is even true for an HP8410 network analyzer system under computer control. With the increased system stability and smaller discretization error, the limits of the HP8510 network analyzer system require even tighter constraints.

CHAPTER 6
CONCLUSION AND RECOMMENDATIONS

This report has presented the fundamental principles and necessary calibration procedures for the accurate measurement of S (Scattering) parameters. These important parameters require a series of steps to properly calibrate a system used to measure the parameters. This is particularly true for measurements made over a broad frequency range for which the usefulness of this parameter set in the design process is ideal. Measurements may be made from below 1 MHz to the millimeter wave spectrum. We have shown the calibration process and standards to be at the heart of such a measurement system.

We have investigated the calibration procedures used by Hewlett–Packard and have found the same anomalies in the resultant data as have other researchers. The purpose of this report has been to investigate the full calibration process for the existing HP measurement system. We begin by reviewing the basic calibration process and measurement system. The approach taken by Hewlett–Packard was discussed as the methods were developed. A full model for the system was also developed. The model was used to develop a full system calibration, including the calibration of the HP "open" circuit reference. This approach has the additional advantage of not requiring the "open" for the calibration, a fact critical to certain measurement environments. In such instances, the calibration must often be done using some alternate procedure such as that presented in this report. More

importantly, the basic formalism of the modeling enables a user to develop a calibration procedure tailored to a specific need where the HP procedure is inadequate. Our premise has been to improve the HP calibration data and then use the fundamental HP procedure when possible. This latter procedure provides a high degree of accuracy if the correct calibration data is available, usually in excess of the accuracy specifications of the HP 8510 network analyzer system.

Sample results have been presented which validate the method and demonstrate the potential errors using HP's process and data. These results have included the effects of both fixed terminations and sliding loads on the choice of calibration data used to represent the HP "open" standard. Limitations of the approach were discussed in addition to assumptions built into the calibration and accuracy process. The final results provide the fundamentals of an accurate calibration process for network analyzer systems. Two basic open reference models were found to give good results. The first model was a 3–term approximation to the open capacitance given by $(0.09183 + 0.000006\ f^2 + 0.0000046\ f^3)$ pF. There should be no linear term as used in the newest of the HP models (in fact no odd terms) to meet with proper synthesis theory which would indicate such terms would represent loss, not capacitance. The 3–order term accounts for neglecting higher order terms. The second model consists of a 0.09135 pF capacitor in series with a 0.000205 μH inductor representing the transmission line effect. These models work well and are recommended.

Additional work is needed to implement of the full calibration process on a Hewlett–Packard or other computer system. Also, no actual work has been done in implementation of the full 2–port calibration process. An obvious extension of this work is to the new measurement environment provided with the HP 8510B network analyzer system. This latter system has incorporated the new process mentioned in

the introduction which avoids difficulties with the source switching. However, the current implementations are known to provide certain fundamental limitations, due to imposed assumptions for simplifying the calibration process. These limitations and the ultimate effects on the calibration of the data require further investigation.

BIBLIOGRAPHY

Adam, S. F. (1984), Microwave instrumentation: An historical perspective, *IEEE Trans. Microwave Theory Tech.*, *MTT*–32(9), pp. 1157–1161.

Brantervik, K. and E. L. Kollberg (1985), A new four port automatic network analyzer: Part 1 – description and performance, *IEEE Trans. Microwave Theory Tech.*, *MTT*–33, pp.563–568.

Brantervik, K. (1985), A new four port automatic network analyzer: Part 1 – theory, *IEEE Trans. Microwave Theory Tech.*, *MTT*–33, pp.569–575.

Braun, C. R. (1983), Software package fully automates scalar network analyzer, *Microwave System News*, pp. 81–93.

Braun, C. R. (1984), Powerful network analyzer refines microwave measurement, *Microwave System News*, pp. 56–64.

Chung, N. S., J. H. Kim, and K. Hong (1987), Error analysis on a six–port ANA by simulation, *IEEE Trans. Instrum. Meas.*, *IM*–36, pp. 496–500.

Cronson, H. M. and L. Susman (1977), A six–port automatic network analyzer, *IEEE Microwave Theory Tech.*, *MTT*–25(12), pp. 1086–1091.

Cronson, H. M. and L. Susman (1981), A dual six–port automatic network analyzer, *IEEE Microwave Theory Tech.*, *MTT*–29(4), pp. 372–378.

Davis, W. A. and D. M. Keller (1988), Calibration of Hewlett–Packard network analyzers – a precision viewpoint, Final report, NASA Langley.

Engen, G. F. and C. A. Hoer (1972), Application of an arbitrary six–port junction to power measurement problems, *IEEE Trans. Instrum. Meas.*, *IM*–21, pp. 470–474.

Engen, G. F. (1973), Calibration of an arbitrary six–port junction for measurement of active and passive circuit parameters, *IEEE Trans. Instrum. Meas.*, *IM*–22, pp. 295–299.

Engen, G. F. (1977a), The six–port reflectometer: an alternative network analyser, *IEEE Trans. Microwave Theory Tech.*, *MTT*–25(12), pp. 1075–1080.

Engen, G. F. (1977b), An improved circuit for implementing the six–port technique of microwave measurements, *IEEE Trans. Microwave Theory Tech.*, *MTT*–25(12), pp. 1080–1083.

Engen, G. F. (1978a), Calibrating the six–port reflectometer, *IEEE MTT–S Int. Microwave Symp. Dig.*, pp. 182–183.

Engen, G. F., C. A. Hoer, and R. A. Speciale (1978b), The application of "thru–short–delay" to the calibration of the dual six port, *IEEE MTT–S Int. Microwave Symp. Dig., pp. 184–185.*

Engen, G. F. (1978c), Calibrating the six–port reflectometer by means of sliding terminations, *IEEE Trans. Microwave Theory Tech., MTT–*26(12), pp. 951–957.

Engen, G. F. and C. A. Hoer (1979), "Thru–reflect–line": An improved technique for calibrating the dual six–port automatic network analyzer, *IEEE Trans. Microwave Theory Tech., MTT–*27(12), pp. 987–993

Franzen, N. R. and R. A. Speciale (1975), A new procedure for system calibration and error removal in automated S–parameter measurements, *Proc. 5th European Microwave Conf.*, pp. 69–73.

Ghannouchi, F. M. and R. G. Bosisio (1988), An alternative explicit six–port matrix calibration formalism using five standards, *IEEE Trans. Microwave Theory Tech., MTT–*36(7), pp. 494–498.

Gledhill, S. (1987), Spectrum analyzer network measurements, *Microwave System News*, pp. 75–84.

Helton, J. W. and R. A. Speciale (1983), A complete and unambiguous solution to the Super TSD multiport calibration problem, *IEEE MTT–S International Symp. Digest*, pp. 251–252.

Hoer, C. A. (1972a), Theory and application of a six–port coupler, *Final Report, NBS* 10757.

Hoer, C. A. (1972b), The six–port coupler: A new approach to measuring voltage, power, impedance, and phase, *IEEE Trans. Instrum. Meas., IM–*21, pp. 466–470.

Hoer, C. A. (1977), A network analyzer incorporating two six–port reflectometers, *IEEE Trans. Microwave Theory Tech., MTT–*25(12), pp. 1070–1074.

Hoer, C. A. (1979), Performance of a dual six–port automatic network analyzer, *IEEE Trans. Microwave Theory Tech., MTT–*27(12), pp. 993–998.

Hoer, C. A. (1981), A high power dual six–port automatic network analyzer used in determining biological effects of RF and microwave radiation, *IEEE Trans. Microwave Theory Tech., MMT–*29, pp. 1356–1364.

Hoer, C. A. (1983), Choosing line lengths for calibrating network analyzers, *IEEE Trans. Microwave Theory Tech., MTT–*31(1), pp. 76–78.

Hoer, C. A. (1987a), On–line accuracy assessment for the dual six–port ANA: Treatment of systematic errors, *IEEE Trans. Instrum. Meas., IM–*36, pp. 514–519.

Hoer, C. A. and G. F. Engen (1987b), On–line accuracy assessment for the dual six–port ANA: Extension to nonmating connectors, *IEEE Trans. Instrum. Meas., IM–*36, pp. 524–529.

Juroshek, J. R. (1987), On–line accuracy assessment for the dual six–port ANA: Experimental results, *IEEE Trans. Instrum. Meas., IM–*36, pp. 520–523.

Judish, R. M. and G. F. Engen (1987), On–line accuracy assessment for the dual six–port ANA: Statistical methods for random errors, *IEEE Trans. Instrum. Meas.*, *IM*–36, pp. 507–513.

Li, S. and R. G. Bosisio (1982), Calibration of multiport reflectometers by means of four open/short circuits, *IEEE Trans. Microwave Theory Tech.*, *MTT*–30(7), pp. 1085–1090.

Pink, J. J. (1987), New scalar network analyzer boasts powerful processing, *Microwave System News*, pp. 8–16.

Somlo, P. I. and J. D. Hunter (1982), A six–port reflectometer and its complete characterization by convenient calibration procedures, *IEEE Microwave Theory Tech.*, *MTT*–30(2), pp. 186–192.

Speciale, R. A. and N. R. Franzen (1976), Accurate scattering parameter measurements on nonconnectable microwave networks, *Proc. 6th European Microwave Conf.*, pp. 210–214.

Speciale, R. A. (1977a), Super TSD. A generalization of the TSD network analyzer calibration procedure, covering n–port measurements with leakage, *IEEE MTT–S International Symp. Digest*, pp. 114–117.

Speciale, R. A. (1977b), A generalization of the TSD network analyzer calibration procedure, covering n–port scattering–parameter measurements, affected by leakage errors, *IEEE Trans. Microwave Theory Tech.*, *MTT*–25(12), pp. 1100–1115.

Speciale, R. A. (1978), Evaluation of Super TSD network analyzer calibration programs by computer simulation, *IEEE MTT–S International Symp. Digest*, pp. 91–93.

Speciale, R. A. (1979), Results of TSD calibrated scattering parameter measurements performed on a commercial ANA, *Proc. 9th European Microwave Conf.*, pp. 210–214.

Speciale, R. A. (1980), Multiport network analyzers, *Report, TRW Defense and Space Systems Group.*

Tippet, J. C. and R. A. Speciale (1982), A rigorous technique for measuring the scattering matrix of a multiport device with a 2–port network analyzer, *IETrans. Microwave Theory Tech.*, *MTT*–30(5), pp. 661–666.

Weidman, M. P. (1977), A semiautomated six port for measuring millimeter–wave power and complex reflection coefficient, *IEEE Microwave Theory Tech.*, *MTT*–25(12), pp. 1083–1085.

Williams, W. L., R. C. Compton, and D. B. Rutledge (1988), Elf: computer automation and error correction for a microwave network analyzer, *IEEE Trans. Instrum. Meas.*, *IM*–37, pp. 95–100.

Woods, D. (1979), Analysis and calibration theory of a general 6–port reflectometer employing four amplitude detectors, *Proc. IEE*, 126, pp. 221–228.

—Hewlett–Packard (1985), Materials Measurement: Measuring the dielectric constant of solids with the HP 8510 network analyzer, *Product Note* 8510–3.

—Hewlett–Packard (1985), Equations for embedding and de–embedding device measurements, *Product Note* 8510–4.

—Hewlett–Packard (1987), Network analysis: Applying the HP 8510B TRL calibration for non–coaxial measurements, *Product Note* 8510–8.

—Hewlett–Packard (1988), Network analysis: Specifying calibration standards for the HP 8510 network analyzer, *Product Note* 8510–5A.

—Hewlett–Packard, Appendix to An analysis of vector measurement accuracy enhancement techniques.

NASA National Aeronautics and Space Administration

Report Documentation Page

1. Report No.	2. Government Accession No.	3. Recipient's Catalog No.
NASA CR-181989		

4. Title and Subtitle	5. Report Date
Calibration of Hewlett-Packard Network Analyzers - A Precision Viewpoint	March 1990
	6. Performing Organization Code

7. Author(s)	8. Performing Organization Report No.
W. A. Davis and D. M. Keller	
	10. Work Unit No. 506-44-21-03

9. Performing Organization Name and Address	11. Contract or Grant No.
Virginia Polytechnic Institute and State University Blacksburg, Virginia 24061	NAS1-18106, Task 9
	13. Type of Report and Period Covered
12. Sponsoring Agency Name and Address National Aeronautics and Space Administration Langley Research Center Hampton, VA 23665-5225	Contractor Report
	14. Sponsoring Agency Code

15. Supplementary Notes

Langley Technical Monitor: C. P. Hearn
Task 9 Final Report

16. Abstract

This report examines alternative calibration procedures for Hewlett-Packard vector network analyzers which lead to an improved open-circuit capacitance model, and hence, higher measurement accuracy.

17. Key Words (Suggested by Author(s))	18. Distribution Statement
vector network analyzer calibration	unclassified - unlimited subject category 32

19. Security Classif. (of this report)	20. Security Classif. (of this page)	21. No. of pages	22. Price
unclassified	unclassified	76	A05